Development of disposable microsensors for plant researches

Md. Abunasar Miah

February 2018

Development of disposable microsensors for plant researches

Md. Abunasar Miah

Doctoral Program in Nanoscience and Nanotechnology

Submitted to the Graduate School of

Pure and Applied Sciences

in Partial Fulfillment of the Requirements

for the Degree of Doctor of Philosophy in

Engineering

at the

University of Tsukuba

Table of contents

Abstract

High salinity has limited the crop yields. Cultivation of the salt-tolerant plant in the saline soil can solve these problems. But, there is still lack of suitable instrumentations to identify the salt tolerant plants. Spectrophotometry, electrical conductivity meter (EC meter), genotypic analysis etc. have been used for identification of salt-tolerant plants. But these methods are expensive, time-consuming, require large volume of samples, complex sample preparation processes, and laboratory based. Alternatively, increasing the production of rice without application of chemical fertilizers, the atmospheric nitrogen fixation is quite interesting. Measurement of dissolved oxygen can ensure us to know the nitrogen fixation mechanism in rice plant, which helps to fix biological nitrogen in rice plants. So, a new inexpensive and easy technique is urgently needed for measuring the dissolved oxygen level in the rice plants. But the measurement of the dissolved oxygen level in the plant is still unclear, due to lack of the proper techniques. Several techniques used but they are expensive and unable to use in the live plant directly. Overall, the main challenges are the development of methods to perform the rapid both laboratory and field-based analyses. These methods must be sensitive and accurate, and able to determine various substances with different properties in 'real-life' samples. Electrochemical sensors are ideally suited for these new applications, due to their high sensitivity and selectivity, portable field-based size, rapid response time and low-cost. Since many electrochemical sensors were conducted in the clinical analyses in a clinical chemistry laboratory but the analysis of the compounds from the live plant is less studied. Therefore, a simple, time-saving, and cost-effective electrochemical sensor were fabricated for the plant applications.

Firstly, microfabricated disposable Na^+ ion-sensing device was developed. Two sets of circular Ag/AgCl electrodes and concentric platinum electrodes were formed on the polyimide base layer. The plastic substarte was used due to the fact of the fabrication cost. To realize such practical devices, stability during storage and reliability of measurements is critical. In microfabricated electrochemical sensing devices of this kind, a deterministic factor for lifespan is Ag/AgCl electrodes used to measured potential difference. We used a thin-film Ag/AgCl electrode structure with a protecting layer along with an additional electrode to grow AgCl in situ before the measurement. The concentric platinum electrodes were used to grow AgCl additionally after the device was completed that ensure longer life span of the Ag/AgCl electrode. Na^+ ion concentration measured using the microfabriated ISEs agreed well with those obtained using the conventional ISEs made with glass capillaries.

Next, a needle-type (type-I) and syringe-needle type (type-II) ion-selective electrodes were fabricated for the measurement of the ion in rice plants. The type-I is formed with a polyimide film, silver, Ag/AgCl, an electrolyte polyvinylpyrrolidone (PVP) layer, and a polyvinylchloride (PVC) coated reservoir. A 0.8 cm length of one end of the silver was used for making the Ag/AgCl electrode. Next, the type-I RE fabrication was followed the type-I ISE fabrication method. Here, a 3 M KCl used for the electrolyte layer and the poly(HEMA) liquid junction was used for the RE. Depending on the experimental purpose, the type-II ISEs were fabricated. Components related to the type-II ISEs are an ion-selective membrane, Ag/AgCl electrode, and internal solution incorporated into a syringe needle (inner diameter: 0.9 mm). The type-II RE was fabricated as like as type-II ISEs. All ISEs are calibrated with the standard solutions. The type-I ISE was applied in the sample solution of the rice plant parts, whereas the type-II ISEs were applied directly into the live rice plant. The obtained results of type-I Na^+ ion-selective electrode and K^+ ion-selective electrode was compared with the inductive coupled plasma atomic emission spectrophotometry (ICP-AES) method.

Finally, a Clark-type oxygen electrode was fabricated to know the level of the dissolved oxygen in solution, gel-sample, soil and live stem of the rice plant. We fabricated a needle-type oxygen electrode (type-I) with an electrolyte layer, oxygen permeable membrane, cathode and anode; and a syringe needle-type oxygen electrode (type-II). A syringe needle (inner diameter: 1.2 mm) was used here. Both oxygen electrodes were characterized in the air saturated state to the Na_2SO_3 saturated state. Although the fabricated oxygen electrode is much smaller than commercialized conventional oxygen electrodes, it showed clear, stable, reproducible responses. While conducting the experiments, however, an unnegligible residual current was detected. The type-I was used in the liquid and solid bacterial medium; and in the soil of the rice root. On the other hand, the type-II was used to measure the dissolved oxygen level in the stem of the live rice plants.

The microfabricated simple and low-cost ion-selective electrodes and the Clark-type oxygen electrodes have demonstrated in this dissertation. The microfabricated all sensing devices could be enhanced the rapid measurement in the field of the agriculture. The developed all sensing device could be a milestone in the field of the plant science. Because the developed sensors are an in-expensive and can be replaced the laboratory based large experimental set-up. The developed sensor can be possible to apply in other plants. Therefore, sensors can be used for the basic research in the plant.

Chapter 1: General Introduction

Foods production needs to increase by 50% globally by the year of 2050 to match the anticipated population growth [1-2]. Simultaneously, the maximum suitable land has already been cultivated and therefore an urgent need for either increase into new cultivable land area or an increase in crop production on standing cultivated lands. The various factors are degraded about 15% world land area, and the drought problem can be solved by the irrigation to increase the productivity of the crops [1], both tasks appear to be rather challenging. The soil salinity is one of the major threats by this end.

Salinity is one of the greatest problems in developing countries due to their low terrain [3, 4]. Natural disaster such as flood can cause the movement of saline water from sea into the cultivable land. The crop production has destroyed by the terrible flood and salinity. Climate change including rising sea level, cyclone and storm are responsible for the loss of the production of crops. According to the Intergovernmental Panel on Climate Change (IPCC), the climate change will continue rising the sea level in the next centuries, even the emission of the greenhouse gas is stable [5]. The sea level is not identical in every geographical area.

Salinity is caused naturally and artificially by irrigation, poor agricultural administration, rising sea-level, flooding, unfertile land, and poor water management. Those factors are drastically reducing the cultivatable land very swiftly. About 1 billion hectares of land are already affected by the salt, which corresponds to approximately 7% of the world area [6]. It has been reported that around 77 million hectares (m ha) of lands are irrigated with sea water, in which 58% of these irrigated lands. Another report estimated that an average 20% of the agricultural lands are already affected by the salt, but this amount increases to more than 30% in countries such as Egypt, Iran, and Argentina [6]. Moreover, the most glycophytes crops cannot survive in the high concentration of the salt. Therefore, the development of the salt tolerance plant is one of the key factor to improve the crop productivity even under high saline condition. Investigation of the salinity level in the plant is important to observe the condition of the plant.

The phenotypic characteristics including plant growth rate [7], biomass weight [8-9], shoot weight [10], leaf Na^+ ion concentration and the ratio of shoot Na^+/K^+ ions [11], and leaf area[12-13] have used for the identification of the salt tolerant plant. The problem of the phenotypic evaluation is time-consuming. In the meantime, several compounds can be measured to identify the salt tolerant plant. These comprise antioxidants [14], ions [15], proteins [16], reactive oxygen species [17-18], and sugar

sugars [19].

Ions are essential micro-nutrients required for the growth of plants. Among those micronutrients, nitrogen (N), phosphorus (P), sodium (Na) and potassium (K) are most important. The plants uptake those nutrients as ionic forms from the soil through the roots by mass flow and diffusion. Ions, especially sodium and potassium ions, are present in the soil as water-soluble, exchangeable, nonexchangeable, and mineral forms. They are important for plants involved in many vegetative metabolic steps such as enzymatic activation, osmosis, carbohydrate production, and cation/anion balance [20]. Although the sodium and potassium are playing an important role in the plant, the excessive level of sodium and potassium ions in the soil has detrimental effect on the plant.

1.1 Salinity researches on plants

Many published papers dealt with salinity over the last four decades. Salinity affected the productivity of crop plants [21]. Though productivity and resistance of plants against pests and diseases have been improved, but the productivity against salinity is still not satisfactory. A relative study of salinity has been done [22] but need more study to make a suitable system for identifying and developing the salinity tolerance plant. The excessive salt in the soil affects flower and stem quality of gerbera daisies [23] and roses (*Rosa hybrida*) [24]. High NaCl concentration in the soil decreases height of bell peppers by 49% (Capsicum annuum L.) and total leaf area by 82% [25]. Salt concentrations higher than 10 mmol L^{-1} (0.58 g L^{-1}) decrease shoot length, leaf area, and dry weight of the plant. The chlorosis, burning of leaf margins and necrosis has occurred at concentrations greater than 50 mmol L^{-1} (2.92 g L^{-1}) NaCl [26]. The chlorophyll contents of *Chrysanthemum indicum* has increased at greater than 100 mmol L^{-1} (5.84 g L^{-1}) and decreased at 150 mmol L^{-1} (8.76 g L^{-1}) [27]. Plant height and crop yields has decreased by the application of NaCl [14]. So that the salt has influenced the crop production and the growth of the plant [28].

Moreover, high salinity in the soil causes several deleterious events in the plant. Ion is accumulated in the plant while excess irrigation done in their root system by the saline water. This saline water is evaporated and precipitated in the leaves [29]. Because, the plant cannot uptake water from the soil due to the presence of excess amount of the salt in the soil [30]. The excess level of the NaCl concentration in the root system of the plant increases intracellular Na^+ and Cl^- concentrations and affects the cellular system [25]. Similarly, the K^+ ion and Ca^{2+} ions are increased in the plant as like as the Na^+ and Cl^- [31-33].

However, the K^+ ion is also critical in the development of salt-tolerant plant. High salinity induces nutritional disorders, especially K^+ ion deficiency. The K^+ ion content in the plant reduced when there was a Na^+ at the plasma membrane, cation channels and transporters. A considerable membrane depolarization has observed while Na^+ pass through the plasma membrane [34]. Therefore, the K^+ cannot pass through the membrane at the same time, which causes the lack of the K^+ ion concentration in the plant. The decreases of the K^+ ion in the cytosol increases the reactive oxygen species (ROS) causing programmed cell death (PCD). To overcome these problem, a deep and longer root system is better for certain plant species to uptake water [35] and/or accumulate osmolytes and osmoprotectants [36], which helps the plant to withstand against osmotic stress condition. However, the salt-tolerant plants survive against the high salt condition by excluding the excess ion or storing the ion in the vacuoles [37-40].

Moreover, the sodium and potassium ions ratio is also important factor to know the mechanism of the salinity tolerance of the plant. In the plant tissues, a significant level of the K^+: Na^+ ratio was decreased with the increases the level of the NaCl [41, 42]. The differences of the ratio are occurred due to the competition of the ions in the root of the soil. The higher uptake of Na^+ will influence the lower uptake of the K^+ ion. Various study on absorption, uptake, root to shoot translocation, and vacuolar sequestration has been conducted to observe the interface between K^+ and Na^+ [38, 43-44]. So, both the Na^+ and K^+ ions has played important role at salinity stress.

1.2 Conventional methods of ion measurement

Plant science is a broad and multidisciplinary topic encompassing plant biochemistry, development, chemical products, and diseases. It includes the production of staple foods (e.g., rice), materials (e.g., timber, oil, rubber, and fiber), genetic modification, environmental management, maintenance of biodiversity, and synthesis of chemicals or raw materials for energy production [45]. Current agriculture demands continuous in-situ information of plant physical and chemical parameters, such as macro-and micro-nutrients, owing to modulation of the amounts of fertilizers to be added. Some commercial systems allow physical data to be obtained, but not much instrumentation has been developed to determine concentrations of key parameters such as nitrogen, phosphorus, sodium and potassium in live pants. These and other parameters are normally obtained by off-line methods [46-49]; these methods provide some data of great accuracy and precision about the soil composition, but they do not allow to measure the ion concentration in the plant.

As a conventional method for the measurement of the concentration of ions, the Kjeldahl digestion method followed by steam distillation was used to measure the total nitrogen content [50]. Piper's method was employed to measure the concentration of Cl^- ions [51]. The total phosphorus content was measured colorimetrically [52, 53]. Calcium and magnesium concentrations were measured by the Versenate method. Turbidimetric method was used to determine the total sulfur content in the sample solution [54]. The root cation exchange capacity was determined by the method reported by [55] which employs acid washing followed by titration of the root-KCl suspension with standard 0.01 KOH solution.

Most research on salinity estimates the amount of elemental Na^+ and K^+ ions at the whole-tissue level (leaves or roots) using techniques such as atomic absorption spectroscopy (AAS), flame photometry (FP) or inductively coupled plasma mass spectrometry (ICP-MS); at the sub-cellular level, techniques such as X-ray microanalysis or secondary ion mass spectrometry (SIMS) can be employed [56]. But, these techniques require large experimental set up, require expensive instruments, labor intensive, complex sample preparation method and manual sampling.

1.3 Impact of oxygen in plants

The molecular oxygen simply referred to as oxygen (O_2) is an important issue for most life forms on earth. It is also an important precursor for producing the nutrient naturally and artificially to the plant. The plant metabolical and physiological responses are depending on the oxygen level [57]. The crop production will be limited if the root system suffered from the oxygen deficiency. The lack of oxygen can be destroyed the function of the roots of the plant.

In the non-legumes plant, the effect of the oxygen deficiency has been studied for long times. For example, the decrease in dissolved O_2 concentration in poor-aerated nutrient solution in hydroponics causes inhibition of root cell division and the decrease in root elongation [58, 59]. Furthermore, the decline in leaf water potential and reduction in stomatal conductance have been found at lower dissolved O_2 concentrations [60,61]. These effects of dissolved O_2 concentration can be considered to relate to root physiological functions such as respiration and water uptake. The water uptake and growth in cucumber plants were analyzed under control of dissolved O_2 concentration [62], and found that decrease in water uptake at lower dissolved O_2 concentrations reduces leaf growth through plant water status. The root respiration in lettuce plants is depressed at lower dissolved O_2 concentrations [63].

In case of legume plant, they are not suffered from the oxygen deficiency. Because, it can utilize the natural oxygen for their growth and productivity. The legumes plants use the oxygen from the environment by using the nodule. A nodule is a globular structure formed on the root of the leguminous plant. The leg hemoglobulin compound found in the nodule which supply the oxygen to the root nodule bacteria to fix the atmospheric nitrogen. In contrast, the non-legumes plant like rice does not have the nodule in their root system and therefore they cannot fix atmospheric nitrogen.

Plants absorb the available nitrogen in the soil through their roots in the form of ammonium and nitrates. The limited bio-availability of nitrogen and the dependence of crop growth on this element have spawned a massive nitrogen-based (N-based) fertilizer industry worldwide [64, 65]. About 60 % of synthetic nitrogen fertilizers are presently used for cereals, with irrigated rice production accounting for approximately 10 % of the use. Since >50 % of the fertilizer applied is actually used by plants, the inefficient use of nitrogen contributes to nitrate contamination of soils and ground water, leading to health hazards and compromising agricultural sustainability. Moreover, manufacturing N-based fertilizer requires six times more energy than that needed to produce either phosphorus or potassium fertilizers [66].

The nitrogen fertilizer has extensively been used as a fertilizer in the production of the rice. The nitrogen fertilizer used in the countries where the production of the rice has been done in the irrigated land rather than in rainfed, upland, or flood-prone lands. For example, the application of the nitrogen fertilizer in South Korea 170 kg N ha^{-1} [67] and in China about 140 kg N ha^{-1}. The increases demand of the using the nitrogen fertilizer will create the pressure on using the fossil fuel. Because the production of the nitrogen fertilizer depends on the fossil fuel. The burning of the fossil fuel has produced green gas to the environment that is harmful for the human being also.

To solve these problem, improvement of the biological nitrogen fixation could be a better way. The biological nitrogen fixation (BNF) to produce nutrients for plant is cost effective and will encourage the farmers to use lower chemical fertilizer. The importance of using BNF is not only related with crop productivity, but also related with the environment. If the farmers realized that the BNF do not reduce the production of the crop, then the use of the chemical fertilizer will drastically reduce. The use of the BNF will save the money that they use for purchasing the chemical fertilizer. However, the environmental benefits of using BNF in rice field are good for health, environmental, and and habitats for aquatic life. Because, the use of the chemical nitrogen fertilizer is runoff to go to the water surface and submerged water. These considerations suggest that the development of sustainable agriculture system for the crop productivity and environment is urgently needed.

In case of rice, it is a non-legumes plant and cannot fix the atmospheric nitrogen. This is due to insufficient supply of the oxygen to the root nitrogen-fixing bacteria. But the rice plants have intercellular spaces interconnected between the shoot and root. Oxygen is supplied to the oxygen-deficient soil through these spaces [68]. This movement of oxygen is occurred by the diffusion process. The diffusion of the oxygen through the plant to the soil is one of the important features. The study of the movement of the O_2 ratio from plant to soil could be the best way to find the production of rice without application of the chemical N-based fertilizers. Because the nitrogen-fixation is depending on the presence of the oxygen. In the rice, the presence of the oxygen is important for the survival of nitrogen-fixing bacteria in the root to fix the atmospheric nitrogen. One of the special feature of the rice plant that can move the oxygen diffuse through the aerenchyma tissues of the stem, leaves and root system to the soil.

In most plant species, diffusion is the mechanism by which O_2 moves. The flow of gases through the through-flow mechanism has used to observe the rate of flow of oxygen in the plant system. The rates of flow are depending on the pressure gradient and aeration system [69, 70]. The pressure gradient may vary depends on the species and environmental conditions. The volume of aerenchyma, organ cross-sectional area and internal anatomy (e.g. presence of diaphragms) are some of the factors that determine resistance at the stem and at root-rhizome junctions. Oxygen that diffuses through pores in plants have been studied in the water lily, and the grass species such as *Phragmites australi)*. The flow of gases due to positive pressures was found in floating-leaved [71] and emergent [69] wetland plants. But the oxygen flows of decreasing in pressure have so far only been studied in *Phragmites australis* [68, 72]. The flow of gases via non-through-flow mechanisms (steady-state condition) have also been proposed i.e., in the rice such as *Oryza sativa* [73]. Also in the submerged plants, the dissolved oxygen produced during the photosynthesis diffuses through a steady-state condition. Even if there is no pathway exists, the oxygen will diffuse due to the increases of the partial pressure of the oxygen [74].

Oxygen also diffuse through the root of the plant. The diffusion of the oxygen in roots is determined by structural, morphological, and physiological features, as well as temperature and demand for O_2 in the rhizosphere. The internal oxygen diffusion depends on the penetration of the roots into the soil [75] and other factors. The wetland species roots have the anatomical features. Depending on the species, some features are expressed constitutively and/or can be enhanced when plants are exposed to low O_2 in the root zone. Moreover, the numbers of adventitious roots of *Rumex* species may be affected by O_2 deficiency [76, 77]. Several structural and morphological features of the O_2 diffusion to the apex of roots in anaerobic condition was done by mathematical modeling.

According to this model, the stele has oxygen diffusion due to the low porosity and relatively high rate of the oxygen consumption [78]. So that the measurement of the diffused O_2 at the plant and soil of plant could be good insight to find the better nitrogen-fixing plant.

1.4 Application of sensors in the agriculture

Sensors can be used to solve the problem of the plant immediately. The sensor is promising tool to develop a modern agriculture. For example, an information on crop, soil, climate, and environmental conditions is possible to known by using the sensor tools. If nutrients in the soil, humidity, solar radiation, density of weeds and all factors affecting the production are known, the use of chemical products such as fertilizers, herbicides, and other pollution products can be reduced considerably. Remote spectral sensing of crops has been intensively investigated and proven to be an important tool in modern agricultural management. Remote spectral sensing has been successfully used to measure crop nutrition, crop disease, water deficiency or surplus, weed infestations, insect damage, plant populations, flood management, and many other field conditions [79-82]. The food quality and contaminants of the food have been detected by using the remote spectral sensing [83-86].

Plants and trees normally release volatile organic compounds (VOCs) as a byproduct of everyday physiological processes. The specific VOCs and the quantities released are indicative of both the crop and field conditions. Humidity, light, temperature, soil condition, fertilization, insects, and plant diseases all affect the release of VOCs. The most common applications of electronic noses in agriculture are to detect crop diseases, identify insect infestations, and monitor food quality. The electronic nose is typically trained by comparing the profile of VOCs released by healthy plants/fruits with diseased plants/fruit. One of the major applications of the electronic nose in the food industry is to assess the freshness/spoilage of fruits and vegetables during the processing and packaging process [87, 88]. Studies have been conducted to detect VOCs that indicate fruit ripeness and/or compounds that trigger fruit ripening, such as ammonia [89], ethanol [90], ethylene [91] and trans-2-hexenal [92]. Electronic noses and electroantennogram sensors have also been used to determine the area of coverage of pheromone traps set to capture insect herbivores [93-95]. Recently, the ability of the electronic nose to identify early stages of insect infestations by detecting VOCs secreted by plants that have been investigated [96, 97].

The wireless sensor, global positioning sensors; soil, water, ion and VOC sensors; microcontroller have been designed and are now under field trials. So that, an efficient sensor system can be important factor for enhancing the crop yield. Due to advances in wireless technologies, wireless sensor networks have been developed, which will enable new precision in agricultural practice. The development of this technology is envisioned to provide revolutionary means for observing, assessing and controlling agricultural practices. Wireless sensor network technology is still in its earliest development stage [98-100].

1.5 Objectives of the study

The main goal of this study was to develop simple, cost effective, and time-saving electrochemical sensors for the plant research. The following devices were developed in this study:

- Disposable Na^+-ion-sensing device for measuring the Na^+ ion directly from the live plants.
- Microfabrication of the needle-type (type-I) and syringe needle-type (type-II) ion-sensing devices for measuring the ionic variation in the rice plants.
- Microfabrication of the Clark-type oxygen electrode for developing a sustainable agriculture system for the rice plants.

References

1. T. J. Flowers: J Exp Bot. **55** (2004) 319.
2. P. Rengasamy: J Exp Bot. **57** (2006) 1023.
3. M.L. Parry, O.F. Canziani, J.P. Palutikof, P.J.van der Linden, and C.E. Hanson: Eds: Climate Change 2007: Impacts, Adaptation and Vulnerability. Contribution of Working Group II to the Fourth Assessment Report of the Intergovernmental Panel on Climate Change, Cambridge University Press, Cambridge, 315-356.
4. IPCC AR4: Intergovernmental Panel on Climate Change (IPCC), Climate Change: 2007 Synthesis Report.

5. M. Ashraf: Crit. Rev. Plant Sci. **13** (1999) 42.

6. R.J. Nicholls, P.P. Wong, V.R. Burkett, J.O. Codignotto, J. E. Hay, R. F. McLean, S. Ragoonaden, and Woodroffe: C.D. Coastal Systems and Low-Lying Areas. **34** (2007) 199.

7. M. Soussi, A. Ocaña, and C. Lluch: J. Exp. Bot. **49** (1998) 1329.

8. N. Geissler, S. Hussin, and H.-W. Koyro: Environ. Exp. Bot. **65** (2009) 220.

9. A. J. Keutgen and E. Pawelzik: Environ. Exp. Bot. **65** (2009) 170.

10. M. Aslam, R. H. Qureshi, and N. Ahmed: Plant Soil **150** (1993) 99.

11. F. Asch, M. Dingkuhn, K. Dörffling, and K. Miezan: Euphytica **113** (2000) 109.

12. S. Akita and G. S. Cabuslay: Plant Soil **123** (1990) 277.

13. L. Zeng, J. A. Poss, C. Wilson, A.-S. E. Draz, G. B. Gregorio, and C. M. Grieve: Euphytica **129** (2003) 281.

14. M. Hanin, C. Ebel, M. Ngom, L. Laplaze, and K. Masmoudi: Front. Plant Sci. **7** (2016) 112.

15. J. A. Hernández, F. J. Corpas, M. Gómez, L. A. d. Río, and F. Sevilla: Physiol. Plant. **89** (1993) 103.

16. J. A. Hernández, M. A. Ferrer, A. Jiménez, A. R. Barceló, and F. Sevilla: Plant Physiol. **127** (2001) 817.

17. I. Kerepesi and G. Galiba: Crop Sci. **40** (2000) 482.

18. N. Sreenivasulu, B. Grimm, U. Wobus, and W. Weschke: Physiol. Plant. **109** (2000) 435.

19. R. Munns, P. A. Wallace, N. L. Teakle, and T. D. Colmer: In Plant stress tolerance: methods and protocols 2010, ed. R. Sunkar (Springer, New York, 2010) pp. 371-381.

20. F. Ghassemi, A. J. Jakeman and H. A. Nix: Canberra, Australia: The Australian National University, Wallingford, Oxon, UK: CAB International (1995).

21. R. Muuns: Plant Cell Environ. **25** (2002) 250.

22. X. Niu, R. A. Bressan, P. M. Hasegawa, and J. M. Pardo: Plant Physi. **109** (1995) 742.

23. D. C. Kreij, C. and T. J. M. van den Berg: Nutrient uptake, production and quality of *Rosa hybrida* in rockwool as affected by electrical conductivity of the plant nutrient solution, p. 519–523. In: Van Beusichem, M.L. (ed.). Plant nutrition-Physiology and applications. Kluwer Academic Publishers, Dordrecht, The Netherlands.

24. K. Chartzoulakis and G. Klapaki: Sci. Hort. **86** (2000) 260.

25. K. Chartzoulakis and M.H. Loupassaki: Agr. Water Mgt. **32** (1997) 225.

26. F. Chen, D. Tholl, J. C. D'Auria, A. Farooq, E. Pichersky and J. Gershenzon: Plant Cell **15** (2003) 494.

27. L. Shabala, T. A. Cuin, I. A. Newman, S. Shabala: J. of EXp. Botany. **14** (2005a) 334.

28. De Kreij, C. and T. J. M. van den Berg.: In: Van Beusichem, M.L. (ed.). Plant nutrition-Physiology and applications. Kluwer Academic Publishers, Dordrecht, The Netherlands. (1990) p. 519–523.

29. K. Chartzoulakis, and G. Klapaki: Sci. Hort. **86** (2000) 260.

30. J. Shalhevet and L. Bernstein: Soil Sci. **106** (1968) 93.

31. D.C. Kreij, and P.C. van: Production and quality of Gerbera in rockwool as affected by electrical conductivity of the nutrient solution. Proc. 7th Intl. Congr. Soilless Culture.

32. D.C Kreij, and P.C. van: Production and quality of Gerbera in rockwool as affected by electrical conductivity of the nutrient solution. Proc. 7th Intl. Congr. Soilless Culture. (1989) p. 255– 264.

33. S. Shabala: J. Exp. Bot. **60** (2009) 712.

34. M. Farooq, A. Wahid, N. Kobayashi, D. Fujita, and S.M.A. Basra: Agron. Sust. Dev. **29** (2009) 212.

35. T. J. Flowers, P. F. Troke, and A. R. Yeo: Annu. Rev. Plant Physiol. **28** (1977) 121.

36. S. Schubert, and A., Läuchli: Plant Soil **123** (1990) 209.

37. S. Schubert, A. Neubert, A. Schierholt, A. Sumer, and A.C. Zörb: Plant Sci. **177** (2009) 202.

38. D.C. Plett, and I.S. Moller: Plant Cell Environ. **33** (2010) 2000.

39. F. J. M. Maathuis and A. Amtmann : Ann. Bot. **84** (1999) 133.

40. S. Shabala, V. Demidchik, L. Shabala, T.A. Cuin, S. J. Smith, A.J. Miller, J. M. Davies, and I. A. Newman: Plant Physiol. **141** (2006) 1665.

41. M. Tester, and R. Davenport: Ann. Bot. **91** (2003) 527.

42. T.A. Cuin, S. Shabala: Plant Cell Physiol. **46** (2005) 1933.

43. M. L. Jackson: Soil chemical analysis. Prentice-Hall, Englewood Cliffs, N. J. (1958) p 498.

44. C.S. Grierson, S.R. Barnes, M.W. Chase, M. Clarke: New Phytol. **192** (2011) 12.

45. M. Y. Kamogawa, A. R. A. Nogueria, M. Miyazawa, J. Artigas, and J. Alonso: Anal. Chim. Acta, **438** (2001) 281.

46. E. Norlin, K. Irgum, and K. E. Ohlsson: Analyst. **127** (2002) 740.

47. P. Masson, C. Morel, E. Martin, A. Oberson, and D. Friensen: Commun. Soil Sci. Plant Anal. **32** (2001) 2253.

48. J. Artigas, A. Beltran, C. Jimenez, A. Baldi, R. Mas, C. Domı´nguez, and J. Alonso: Comput. Electron. Agric. **31** (2001) 293.

49. Piper: Soil and plant analysis. Interscience, New York. (1947) p 368.

50. R. E. Kitson, and M. G. Mellon: Ind. Eng. Chem. Anal. Ed. **16** (1944) 383.

51. C. J. Barton: Anal. Chern. **20** (1948) 1073.

52. L. Chesnin, and C. H. Yien: Soil Sci. Soc. Am. Proc. **15** (1950) 151.

53. W. M. Crooke: Pl. Soil. **21** (1964) 49.

54. F. Licausi, F.M. Giorgi, E. Schmälzlin, B. Usadel, P. Perata, J.T. Van Dongen, P. Geigenberger: Plant Cell Physiol. **52** (2011) 1972.

55. S. Akita and G. S. Cabuslay: Plant Soil **123** (1990) 277.

56. H. Rolletschek Stangelmeyer and A. Borisjuk: Sensors 9 **(**2009) 3227.

57. C. Chun and T. Takakura: Environ. Control in BioI. **32** (1994) 135.

58. S. R. Stachowiak M. and E. Van Volkenburgh: Exp. Bot**. 40** (1989) 94.

59. J. A. Lockhart: Theor. BioI. **8** (1965) 275.

60. S. Yoshida, M. Kitano and H. Eguchi: Environ. Control in BioI. **34** (1996) 58.

61. C.E. Jeffree J.E. Dale and S.C. Fry: Protoplasma **132** (1986) 98.

62. M. 1. Gimenez-Abian, D. L. C. Torre, and J. F. L. pez-Saez: Environ. Exp. Bot. **27** (1987) 237.

63. A. Dobermann: Proceedings of the IFA International Workshop on Fertilizer Best Management Practices. Fertilizer Best Management Practices. Brussels, Belgium: International Fertilizer Industry Association. Nutrient use efficiency-measurement and management in a time of new challenges. (2007) p 28.

64. Westhoff: The economics of biological nitrogen fixation in the global economy. In: Emerich DW, Krishnan HB, editors. Nitrogen fixation in crop production. Madison, WI: American Society of Agronomy. Agronomy Monograph. (2009) p 328.

65. D. J. G. Silva, G. E Serra, J. R. Moreira, J. C. Goncalves and J. Goldenberg: Crops Science. **210** (1978) 906.

66. S. Pandey: Nutrient management technologies for rainfed rice in tomorrow's Asia: economic and institutional considerations. In: Ladha JK, Wade L, Dobermann A, Reichardt W, Kirk GJD, Piggin C, editors. Rainfed lowland rice: advances in nutrient management research. Proceedings of the International Workshop on Nutrient Research in Rainfed Lowlands, 12-15 Oct. 1998. Ubon Ratchathani, Thailand. Manila (Philippines): International Rice Research Institute. (1998) p 28.

67. H. B. Sifton: Air-space tissue in plants. Botanical Review. **11** (1945) 143.

68. Brix H., B.K. Sorrell and P.T. Orr: Internal pressurization and convective gas flow in some emergent freshwater macrophytes (1992).

69. J. Armstrong, W. Armstrong, P. M. Beckett, J. E. Halder, S. Lythe, R. Holt and A. Sinclair (Cav.) Trin. Ex Steud. Aquatic Botany. **54** (1996) 197.

70. J. L. Schuette, and M. J. Klug: Plant Physio. **108** (1995) 1258.

71. J. L. Schuette, M. J. Klug, and K. L. Klomparens: Plant, Cell and Environment. **17** (1994) 365.

72. J. Armstrong W. Armstrong and P.M. Beckett: New Phytologist, **120** (1992) 207.

73. W. Armstrong: Advances in Botanical Research. **7** (1979) 332.

74. E. J. W. Visser, G. M. Bogemann, C. W. P. M. Blom and L. A. C. J. Voesenek: Journal of Experimental Botany. **47** (1996) 410.

75. P. Laan, M. J. Berrevoets, S. Lythe, W. Armstrong and C. W. P. M. Blom: Journal of Ecolog. 77 (1989) 703.

76. B. K. Sorrell: Australian Journal of Marine and Freshwater Res. **45** (1994) 1541.

77. J. Gibbs, D.W. Turner, W. Armstrong, M.J. Dawent, and H. Greenway: Australian Journal of Plant Physio. **25** (1998) 758.

78. B. K. Sorrell: Australian Journal of Marine and Freshwater Research. **45** (1994) 1541.

79. I. M. Scotford and P. C. H. Miller: Biosyst. Eng. **90** (2005) 235.

80. M. Govender, K. Chetty, and H. Bulcock: Water SA. **33** (2007) 145.

81. J. Sanyal and X. X. Lu: Nat. Hazards. **33** (2004) 283.

82. M. Govender, P. J. Dye, I. M. Weiersbye, E. T. F. Witkowski and F. Ahmed: Water SA. **35** (2009) 741.

83. A. F. Bin Omar and M. Z. Bin: Int. J. Comput. Elect. Eng. **1** (2009) 1793.

84. K. Katayama, K. Komaki and S. Tamiya: Hortscience. **31** (1996) 1003.

85. A. Garrido, M. T. Sanchez, G. Cano, D. Perez and C. Lopez: J. Food Quality. **24** (2001) 539.

86. A. M. K. Pedro and M. M. C. Ferreira: Anal. Chem. **77** (2005) 2505.

87. A. K. Deisingh, D. C. Stone and M. Thompson: Int. J. Food Sci. Tech. **39** (2004) 587.

88. I. A. Casalinuovo, D. Di Pierro, M. Coletta and P. Di Francesco: Sensors. **6** (2006) 1428.

89. P. Ivanov, E. Llobet, A. Vergara, M. Stankova, X. Vilanova, J. Hubalek, I. Gracia, C. Cane and X. Correig: Sens. Actuators B. **111** (2005) 63.

90. P. Ivanov, E. Llobet, A. Vergara, M. Stankova, X. Vilanova, J. Hubalek, I. Gracia, C. Cane, and X. Correig: Sens. Actuators B. **111** (2005) 63.

91. C. Baratto, G. Faglia, M. Pardo, M. Vezzoli, L. Boarino, M. Maffei, S. Bossi and G. Sberveglieri: Sens. Actuators B. **108** (2005) 278.

92. U. Herrmann, T. Jonischkeit, J. Bargon, U. Hahn, Q. Y. Li, C. A. Schalley, E. Vogel and F. Vogtle: Anal. Bioanal. Chem. **372** (2002) 611.

93. T. C. Baker and K. F. Haynes: Physiol. Entomol. **14** (1989) 102.

94. A. E. Sauer, G. Karg, U. T. Koch, J. J. Dekramer and R. Milli: Chem. Senses. **17** (1992) 543.

95. S. Schutz, B. Weissbecker and H. E. Hummel: Biosens. Bioelectron. **11** (1996) 427.

96. A. H. Purnamadjaja and R. A. Russell: Autonomous Robots. **23** (2007) 113.

97. W. G. Henderson, A. Khalilian, Y. J. Han, J. K. Greene and D. C. Degenhardt: Comput. Electron. Arg. **70** (2010) 157.

98. L. Ruiz-Garcia, P. Barreiro, J. Rodriguez-Bermejoz and J. I. Robla: Spanish J. Agr. Research. **5** (2007)142.

99. L. Ruiz-Garcia, L. Lunadei, P. Barreiro and J. I. Robla: Sensors. **9** (2009) 4728.

100. D. J. Greenwood, K. Zhang, H. W. Hilton and A. J. Thompson: J. Agr. Sci. **148** (2010) 259.

Chapter 2: Disposable Na^+ Ion-Sensing Device for Research on Salt-Tolerant Plants

2.1 Introduction

Concentration of Na^+ ions within plants were measured by techniques including atomic absorption spectrophotometry [1], flame photometry [2], plasma spectrometry [3], and ^{23}Na-NMR microscopy [4]. However, they require a large volume of sample solution and expertise. In addition, these techniques are invasive and require an expensive instrument. As simple inexpensive instruments, portable electric conductivity meter (EC meter) are used. However, a problem with this method is that the measurement is not specific; the EC meter responds to all ionic species in the solution. Also, fluorescence measurement is often used in basic researches [5]. However, a problem is that fluorescent dyes are chemically invasive.

To solve these problems, a glass capillary ion-selective electrodes (ISEs) were used for the measurement of the Na^+ ion concentration in the plant cells [6-8]. However, the preparation of the glass capillary ISEs requires expertise, collection of materials and reagents, and special instruments. Therefore, if Na^+ ion concentration can be measured immediately using an inexpensive disposable Na^+ ion-sensing device, it will be a great advantage.

An issue for the practical application of devices of this kind is stability during long-term storage and reliability of measurements. In microfabricated electrochemical sensing devices of this kind, a deterministic factor for lifespan is the Ag/AgCl electrodes used to measure potential difference. To this end, we have used a thin-film Ag/AgCl electrode structure with AgCl grown from pinholes in a protecting layer. In addition, an additional electrode was formed to grow AgCl in situ before the measurement [10] or even after completing the device. In this study, we fabricated a disposable Na^+ ion-sensing device to measure Na^+ ion concentration directly from the stem of the Welsh onion. Composition of data with those obtained using glass capillary ISEs demonstrated that our device can be research for on salt-tolerant plants.

2.2 Experimental procedure

2.2.1 Reagents and materials

Materials and reagents used for the fabrication and characterization of the devices werepurchased from the following commercial sources: a polyimide sheet (130 μm thick) from JMT Corporation (Osaka, Japan); a polyvinylchloride (PVC) sheet (120 μm thick) from As One Corporation (Osaka, Japan); a positive photoresist (S-1818G) from Dow Chemical (Midland, MI, USA); soda lime glass capillaries (external diameter: ~1.8 mm, internal diameter: ~1.5 mm) from Asahi Glass (Tokyo, Japan); bis(12-crown-4) and 2-nitrophenyloctyl ether (NPOE) from Dojindo (Kumamoto, Japan); sodium tetraphenylborate from Sigma Aldrich (Buchs, Switzerland); agarose S from Nippon Gene (Toyama, Japan); a silver wire (diameter: 1 mm) from The Nilaco Corporation (Tokyo, Japan); an adhesive, Aron Alpha®, from Toagosei (Tokyo, Japan). PVC powder, tetrahydrofuran (THF), and other reagents were purchased from Wako Pure Chemical Industries (Osaka, Japan). The Welsh onion was obtained from a local supermarket. Solutions were prepared with Milli-Q water (Millipore, Tokyo, Japan).

2.2.2 Microfabrication of the Na^+ ion-sensing device

The microfabricated Na^+ ion-sensing device consisted of a Na^+ ISE and a RE. The device was constructed with polyimide and PVC layers with electrodes and solution reservoirs (Fig. 2.1). We used plastics considering the fabrication cost and the necessity of the deformation of the device when it is placed and fixed on a part of a plant. Two sets of circular Ag/AgCl electrodes and concentric platinum electrodes were formed on the polyimide base layer. The Ag/AgCl electrodes were used to measure the potential of the ISE, whereas the concentric platinum electrodes were used to grow AgCl additionally *in situ* after the device was completed. Reservoirs for the electrolyte solutions of the ISE and the RE were formed by making through-holes in the second polyimide layer, which was bound to the base layer using the adhesive. The top PVC layer with a Na^+ ion-selective membrane and the through-hole for the liquid junction of the RE was bound to the second polyimide layer.

The electrodes were formed by a thin-film process. A 30-nm-thick chromium layer and a 300-nm-thick platinum layer were sputter-deposited in this order on the polyimide base layer after the formation of positive photoresist patterns, and the electrode patterns were formed by lift-off. The chromium layer was used to promote the adhesion of the platinum layer to the base layer. Then, 600-nm-thick silver patterns were formed only on the two circular platinum areas by lift-off in the same manner.

The positive photoresist was also used for insulation and three pinholes of 40 μm diameter were

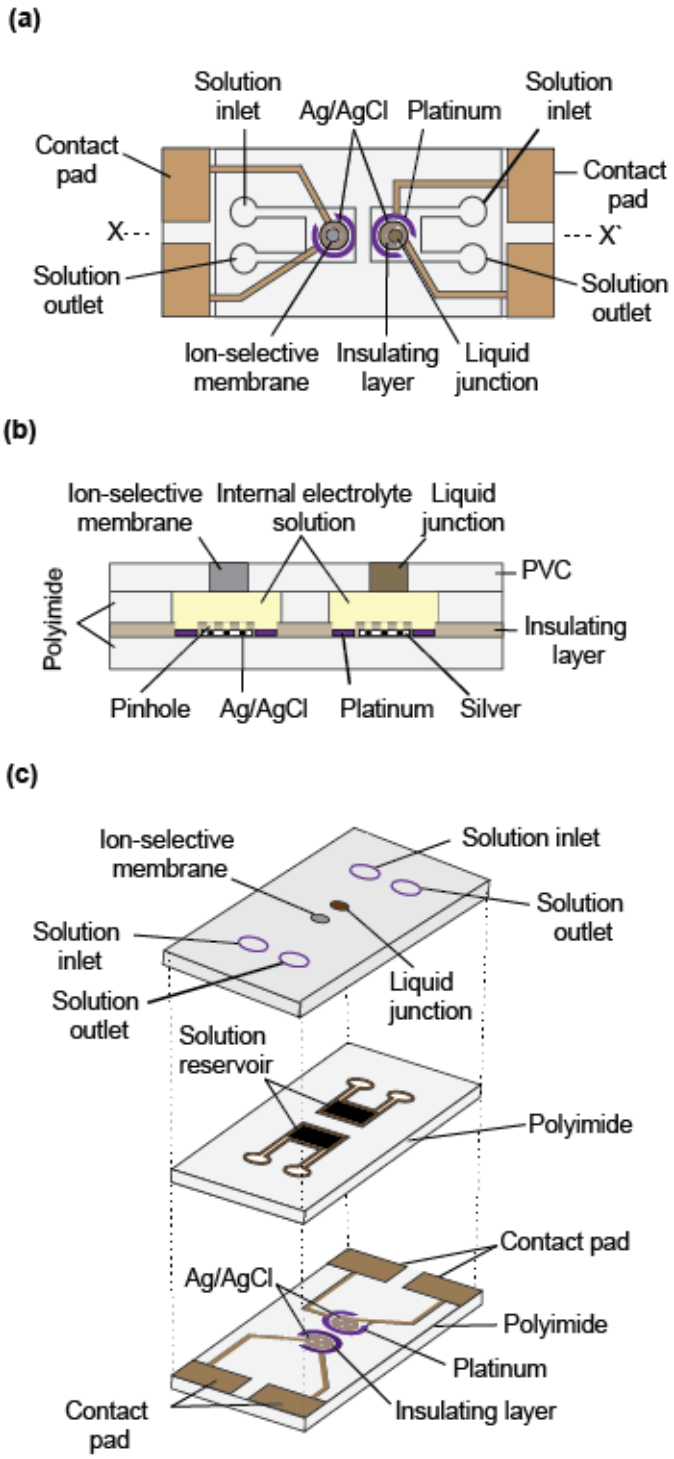

Fig. 2.1 Construction of the microfabricated Na^+ ion-sensing device. (a) Top view. (b) Cross section of the ISE and RE regions along the line X-X'. The thicknesses are not to scale. (c) Exploded view.

formed on each circular silver electrode**.** The thickness of the insulating layer was 2.7 μm. Next, a100 mM KCl solution was placed on the silver pattern and the concentric platinum pattern, and AgCl was grown from the pinholes into the silver layer by applying a constant current (50 nA) for 10 min using a galvanostat (HA-151, Hokuto Denko, Japan) [10]. After the device was completed and used for experiments, AgCl was additionally grown using the internal electrolyte solution (1.0 M KCl) by applying 50 nA for 5 min in the same manner to guarantee the stable potential of the Ag/AgCl electrode.

For the Na^+ ion-selective membrane, crown ether is a representative ionophore [11]. To form the membrane, 101 mg of PVC powder was dissolved in 3 mL of THF. Then, 200 μL of NPOE, 10 mg of bis(12-crown-4), and 6 mg of sodium tetraphenylborate were added. The mixture was thoroughly stirred and 2 μL of the solution was injected into one of the through-holes (diameter: 1 mm) formed in the PVC layer before adhering it to the underlying polyimide layer. Before the injection, the bottom of the through-hole was closed with a sticky note paper, which was removed after the membrane was formed. The PVC substrate with an ion-selective membrane was stored at room temperature for 24 h and was fixed to the polyimide layer using an adhesive.

To make the liquid junction for the RE, a 2% agarose gel solution was prepared with a 1.0 M KCl solution. The solution was heated on a hot plate for 30 min at 90 °C and was injected into the other through-hole of the PVC layer without the ion-selective membrane after bonding the PVC layer to the second polyimide layer.

To complete the Na^+ ion-sensing device, a 1.0 M KCl solution was injected into the reservoirs for the ISE and the RE as internal electrolyte solutions using a micropipette. The solutions were replenished with fresh solutions every time before conducting the new experiment.

2.2.3 Fabrication of the glass capillary ISE and RE

Na^+ ISE~~s~~ were also made with a glass capillary by an established technique and used for comparison as a reliable device. It consisted of a soda lime glass capillary, an ion-selective membrane formed at one end, a Ag/AgCl electrode, and an internal filling solution. One end of the glass capillaries was made thinner (inner diameter: ~1 mm) using a puller (Narishige, Japan).

In forming the ISE, the glass capillary was washed with distilled water and dried overnight in a covered plastic box. The materials used for the ion-selective membrane were the same as those used

for the microfabricated ISE. To form the ion-selective membrane, the end of the glass capillary was immersed in the mixture containing the ionophore and was removed. After that, the capillary was kept in a plastic box overnight. The Ag/AgCl electrode was made by immersing a silver wire in a 100 mM KCl solution and growing AgCl on the surface by applying 250 μA for 10 min using the galvanostat. The AgCl area was 0.8-cm long. Finally, the glass capillary with the ion-selective membrane was filled with a 1.0 M KCl solution, and the Ag/AgCl wire was inserted there so that only the part covered with AgCl contacted the solution.

The RE for the glass capillary ISE was fabricated in the same manner. It consisted of a glass capillary with a liquid junction and a Ag/AgCl electrode immersed in an electrolyte solution. The glass capillary with a smaller diameter at the end was prepared as the one used for the ISE. An agarose gel (2%) containing 1.0 M KCl was used for the liquid junction. The agarose solution was heated on the hot plate for 30 min at 90 ºC, and the end of the glass capillary was filled with an electrolyte gel by dipping its end into the solution. Finally, the Ag/AgCl wire was inserted into the capillary, and a 1.0 M KCl solution was introduced into the glass capillary to complete the RE. When not in use, the glass capillary ISE and RE were stored in a plastic box after gently cleaning them with distilled water and wiping with tissue paper.

2.2.4 Characterization of the devices

The response profile of the microfabricated ISE was obtained with NaCl standard solutions. One of the solutions was placed on the chip to cover the ion-selective membrane and the liquid junction. After the potential was stabilized, the solution was discarded, and the ion-selective membrane and the liquid junction were cleaned with distilled water and dried with tissue paper. Then, the next solution was placed there. The same steps were repeated for all solutions.

The stability of the microfabricated Ag/AgCl electrode was checked in a 1.0 M KCl solution in a beaker. A commercial Ag/AgCl electrode (2060A, Horiba) was immersed there. A 3.3 M KCl solution was used for the internal solution of the commercial electrode. The potential of the microfabricated Ag/AgCl electrode was measured with respect to the commercial electrode.

2.2.5 Measurement of Na^+ ion concentration in Welsh onion

For both types of ISEs, the potential of the ISE was measured with respect to the corresponding RE using an electrometer (AutoLab PGSTAT12, Eco Chemie, Utrecht, Netherland). For pre-conditioning, the ISE was immersed in a 100 mM NaCl solution for 30 min. The ion-selective membrane and the liquid junction were cleaned with distilled water before and after the experiments. To use it in other days, the microfabricated device was rinsed with water, gently dried with tissue paper, and kept in a plastic box with a cover. Between measurements with the same Welsh onion sample, ISE membrane on the device was dipped in the 100 mM NaCl solution.

Welsh onion was selected as model plan**t.** Welsh onion was purchased from a local supermarket of Tsukuba, Japan. Purchased Welsh onion and salt exposed Welsh onion were used for this study. For the latter, the roots of Welsh onions were immersed continuously in a 100 mM NaCl solution in a beaker and the solution was replaced with a fresh one every 2 days. The Na^+ ion concentration was measured at several locations, which was indicated as distances from the bulb of the Welsh onion (Fig. 2.2 (a)). Both sides of the same Welsh onion were used for the measurement using both microfabricated and glass capillary ISEs. For the microfabricated ISE, a part of the stem surface of the Welsh onion was peeled off (Fig. 2.2 (a)), and the ISE and RE areas were attached and fixed there by applying pressure slightly by hand (Fig. 2.2 (b)).

The areas used for the measurement for the microfabricated ISE and RE were closed with a polyimide tape and the locations used for the glass capillary ISE and RE were prepared on the other side of the same Welsh onion by scratching the surface slightly. The glass capillary ISE and RE were inserted there (Fig. 2.2 (b) and (c)).

The Welsh onions were discarded every time after measurement at all locations. The Na^+ ion concentration was calculated on the basis of the calibration plot obtained with NaCl standard solutions. The internal solutions of the ISE and RE for both the microfabricated device and the glass capillary electrodes were replenished with a fresh solution every time prior to the measurement. The experiments were conducted at 25 °C.

2.3 Result and Discussion

2.3.1 Performance of the Na^+ ion-sensing device

The adhesion of the platinum and silver electrodes to the underlying layer was sufficient even after immersion in a 1.0 M KCl solution for at least 8 days. The stability of the potential of the thin-

(a)

(b)

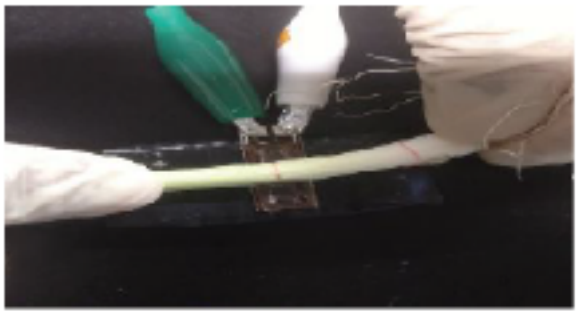

(c)

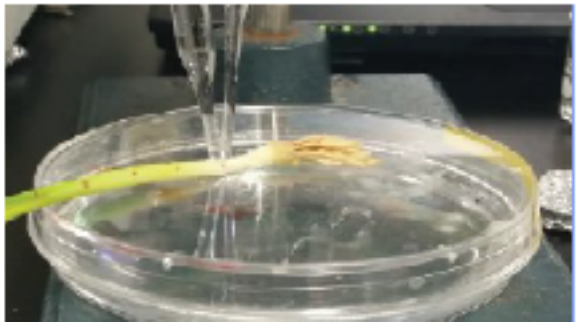

Fig. 2.2 Measurement of Na^+ ion concentration. (a) A predetermined part of the Welsh onion was peeled off for the measurement using the microfabricated Na^+ ion-sensing device. (b) A part of the Welsh onion is placed on the ion-selective membrane and liquid junction of the microfabricated Na^+ ion-sensing device and slight pressure is applied. (c) For the glass capillary ISE and RE, a part of the Welsh onion was scratched, and the electrodes were inserted there.

film Ag/AgCl electrode was checked in the same 1.0 M KCl solution used for the internal electrolyte solution. The potential could be maintained for at least 2.5 h accompanying a gradual drift in the negative direction (–2 mV). Therefore, by reproducing AgCl prior to each measurement, reliable measurements can be conducted.

Fig. 2.3 (a) shows the response profile of the microfabricated ISE when the standard NaCl solution on the chip was changed sequentially. The potential was shifted in the positive direction with the increase in Na^+ ion concentration. Fig. 2.3 (b) shows the relationship between the measured potential and the Na^+ ion concentration of the microfabricated and glass capillary ISEs. As anticipated from the Nernst equation, a linear relationship was observed for both cases in the examined concentration range. The slopes of the plots for the microfabricated ISE and the glass capillary ISE were +55.1 and +55.4 mV/decade, respectively, and was slightly smaller than the expected value at 25 °C (+59.2 mV/decade). The values obtained with the two types of ISE were close, demonstrating that the microfabricated ISE along with the integrated RE can be used like the conventional ISE and RE made with glass capillaries.

2.3.2 Measurement of Na^+ ion concentration in Welsh onion

In this study, Welsh onion was used as model plant. Although the device worked normally for measurements over several days, we used a new one when we judged that the output became unstable. The performance of the devices used was essentially the same as that mentioned in the Section 2.2.3 and no significant difference was observed. Two types of live Welsh onion were used. One was as purchased from the supermarket and was not exposed with the salt. As for the other one, the root was exposed to 100 mM NaCl. Changes in the Na^+ ion concentration was monitored for the two types of Welsh onion using the microfabricated Na^+ ion-sensing device and the glass capillary ISEs (Figs. 2.4 and 2.5). The concentration of Na^+ ions increased in all locations of Welsh onion as time elapsed but decreased as the location was distant from the root. The measured concentrations were very close between the microfabricated device and the glass capillary device. The tendency agrees with that of similar experiments conducted with rice [12], onion [13], and sorghum [14].

2.4 Conclusion

The microfabricated ISE is applicable to the direct measurement of Na^+ ion concentration without

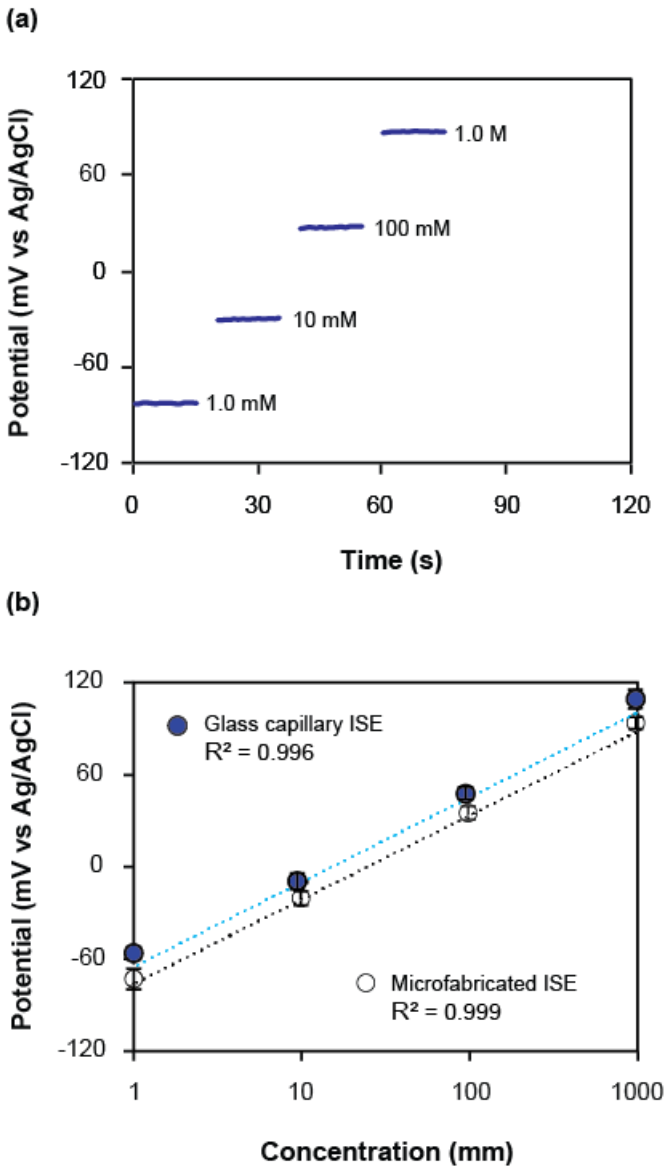

Fig. 2.3 Response of the microfabricated ISE obtained with NaCl standard solutions. (a) Response profile recorded when the standard solution on the sensitive area was changed. The parts while exchanging the solution are omitted. (b) Dependence of the potential of the ISE on the concentration of Na^+ ions. For reference, the calibration plot for the glass capillary ISE is also shown. Averages and standard deviations are shown (n = 5), although most of the error bars are behind the symbols.

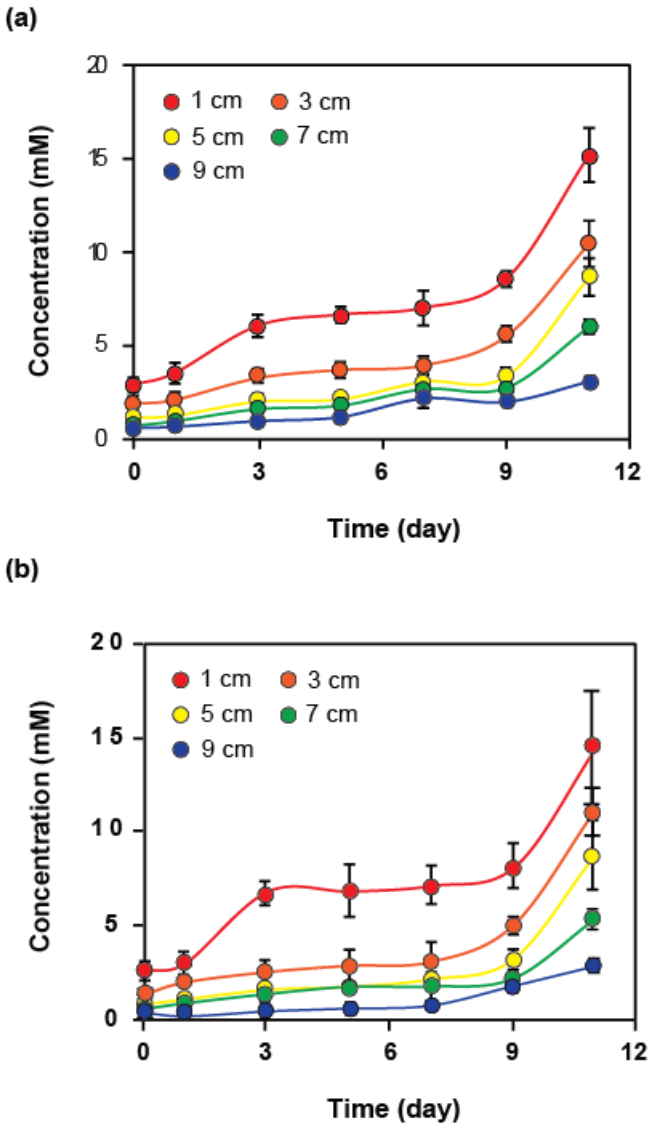

Fig. 2.4 Time courses of Na^+ ion concentration measured at five locations of Welsh onion. The root of the Welsh Onion was immersed in a 100 mM NaCl solution continuously. (a) Changes obtained using the microfabricated ISE. (b) Changes obtained using the glass capillary ISE. In (a) and (b), the lines are guides for the eyes.

pinhole formed in the insulating layer. The AgCl can be grown repeatedly prior to measurements using a platinum electrode formed within the same solution reservoir even after the device was completed. The electrodes actually provided the potential as expected in a Ag/AgCl electrode for a sufficiently long time needed for measurements. The Na^+ ion concentration measured using the microfabricated ISEs agreed well with those obtained using the conventional ISEs made with glass capillaries. Changes at different times and locations of the Welsh onion could be measured clearly. On the basis of this technique, ion-sensing devices for other ions can also be realized. This device will be a useful tool for the efficient screening of salt-tolerant plants.

References

1. R. Munns, P. A. Wallace, N. L. Teakle, and T. D. Colmer: In Plant stress tolerance: methods and protocols 2010, ed. R. Sunkar (Springer, New York, 2010) p. 371-381.
2. R. K. Rabie and K. Kumazawa: Soil Sci. Plant Nutr. **34** (1988) 375.
3. D. Jha, N. Shirley, M. Tester, and S. J. Roy: Plant Cell Environ. **33** (2010) 793.
4. S. Olt, E. Krötz, E. Komor, M. Rokitta, and A. Haase: J. Magn. Reson. **144** (2000) 297.
5. S. J. Halperin and J. P. Lynch: J. Exp. Bot. **54** (2003) 2035.
6. D. E. Carden, D. Diamond, and A. J. Miller: J. Exp. Bot. **52** (2001) 1353.
7. D. E. Carden, D. J. Walker, T. J. Flowers, and A. J. Miller: Plant Physiol. **131** (2003) 676.
8. S.-K. Lee, W. F. Boron, and M. D. Parker: Sensors. **13** (2013) 984.
9. H. Suzuki, A. Hiratsuka, S. Sasaki, and I. Karube: Sens. Actuators B. **46** (1998) 104.
10. H. Suzuki and T. Taura: J. Electrochem. Soc. **148** (2001) E468.
11. P. Bühlmann, E. Pretsch, and E. Bakker: Chem. Rev. **98** (1998) 1593.
12. M. A. Razzaque, N. M. Talukder, M. T. Islam, and R. K. Dutta: Arch. Agron. Soil Sci. **57** (2011) 33.
13. M. C. Shannon and C. M. Grieve: Sci. Hortic. **78** (1999) 5.

14. G. W. Netondo, J. C. Onyango, and E. Beck: Crop Sci. **44** (2004) 797.

Chapter 3: Microfabrication of the Needle-Type Ion-Selective Electrodes for Researches on Salt Tolerant Rice Plants

3.1 Introduction

An electrochemical sensor can be defined as a device that transforms chemical reaction information of the analyte into electrical signal and recorded by an instrument. The potentiometric ion-selective electrodes (ISEs) respond to the activity of the analyte ions. The potential of the ISEs changes in proportion to the logarithm of the activity. As the ion-selective membranes, glass [1], plasticized polymers [2], or various crystalline materials have been used. A representative is probably the pH glass electrode which is still one of the most important standard laboratory devices. On the other hand, the ion-selective electrode is usually made from an organic polymeric matrix containing an ionophore, a lipophilic ligand, and a lipophilic ionic species. The pH glass electrode guarantees the operation of the ISE by keeping the total amount of measuring ions inside the membrane constant, while the ion-selective electrode assures a selective response of the ISE to the target ion. ISEs are cheap and simple devices that can be miniaturized easily, allowing on-line and in-situ measurements and may provide speciation information.

In the plant research, ion-selective electrodes will be useful. Some micro-sensors are available, but they used in the sample solution only. The measurement of the ion directly from the plant is less studied. Although ion-selective electrodes made with glass capillaries are used particularly for physiological researches, special care is needed for handling because they are easily broken. To meet these requirements, we newly developed a needle-type Na^+ and K^+ ion-selective electrodes that can measure ion concentrations in live plants directly.

3.2 Experimental Section

3.2.1 Reagents and materials

Material and reagents used for the fabrication and characterization of the devices were purchased from the following commercial sources: a polyimide sheet (130 μm thick) from JMT Corporation (Osaka, Japan); a positive photoresist from Dow Chemical (Midland, USA); bis(12-crown-4) and 2-nitrophenyloctyl ether (NPOE) from Dojindo (Kumamoto, Japan); valinomycin, dibutyl sebacate

(DOS), tetrahydrofuran (THF), polyvinylpyrrolidone (PVP), polyvinyl chloride (PVC) powder, potassium chloride (KCl), and sodium chloride (NaCl) from Wako Pure Chemical Industries (Osaka, Japan); sodium tetraphenylborate, poly(HEMA) poly(2-hydroxyethyl methacrylate) (poly(2-hydroxyethyl methacrylate)), and potassium tetrakis (4-chlorophenyl) borate (KTpClPB) from Sigma Aldrich (Buchs, Switzerland). Syringe needles (0.9 mm in inner diameter) were purchased from Terumo (Tokyo, Japan). Solutions were prepared with Milli-Q water (Millipore, Tokyo, Japan).

3.2.2 Microfabrication of the needle-type and syringe needle-type Na^+ and K^+ ion-sensing devices

The needle-type (type-I) and syringe needle-type (type-II) microfabricated Na^+ and K^+ ion-selective electrodes (ISEs) consisted of indicator electrodes and reference electrodes (REs). The fabrication process of the type-I ISEs and the reference electrode are outlined in Fig. 3.1.

The structure of the type-I ISE is shown in Fig. 3.2. The type-I ISE device was constructed with a polyimide film, silver, a polyvinylpyrrolidone (PVP) layer (act as an electrolyte layer) and a polyvinylchloride (PVC) layers as a reservoir for the ISEs (Fig. 3.2). The polyimide film was used as a substrate considering the fabrication cost. The Ag/AgCl electrode was formed at one end of the silver layer (0.8 cm long) by depositing AgCl. The Ag/AgCl electrodes were used to measure the potential of the ISEs.

To prepare the electrolyte solution for the Na^+ ion-selective electrode, a 75 % PVP solution was prepared by dissolving the PVP powder in a 0.1 M NaCl solution. The Ag/AgCl part of the electrode was immersed in the 75% PVP solution and was removed from the solution immediately. The dry PVP layer was obtained after drying for 30 min. THF was used as a solvent for making a 66% PVC solution. The electrode with the PVP layer was immersed in the PVC solution to make the reservoir of the electrolyte layer. The PVC-coated electrodes were formed after drying for 10 min. After forming the electrolyte chamber, the end of the Ag/AgCl electrode was cut using a scissor. The Na^+ ion-selective membrane was formed at the end by immersing the part in the Na^+ ion-specific ionophore solution. The membrane was formed after drying for at least 24 h.

Similarly, the preparation of the type-I K^+ ion-selective electrode was followed the preparation of the type-I Na^+ ion-selective electrode. A 0.1 M KCl solution and K^+ ion-selective membrane was used here. In case of the type-I RE, the internal solution and the membrane of the type-I Na^+ ion-selective electrode was replaced with the 3 M KCl solution and the poly(HEMA) liquid junction. The

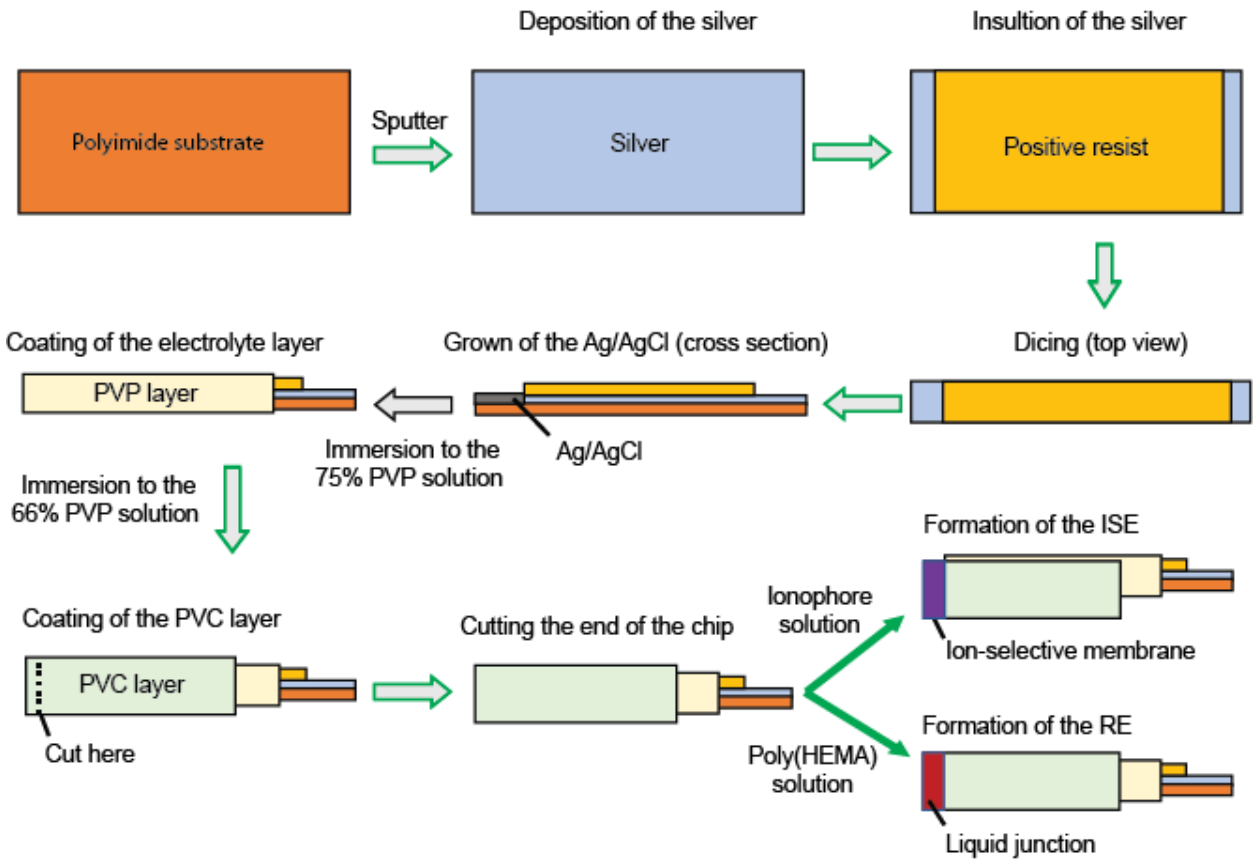

Fig. 3.1 The steps involved for making the electrolyte layer of the electrodes. The PVP solution was dissolved in internal solution. The PVP was dissolved in the 0.1 M NaCl for the the Na^+ ion-selective electrode, 0.1 M KCl for the K^+ ion-selective electrode, and 3M KCl for the RE. Then, AgNO3 solution was added to the electrolyte solution for getting the expected potential during the experiment. The prepared electrode can be used as Na^+ ion-selective electrode, K^+ ion-selective electrode and RE by dipping the end in the Na^+ ion-specific solution, K^+ ion- specific solution, and poly(HEAM) liquid junction solution, respectively.

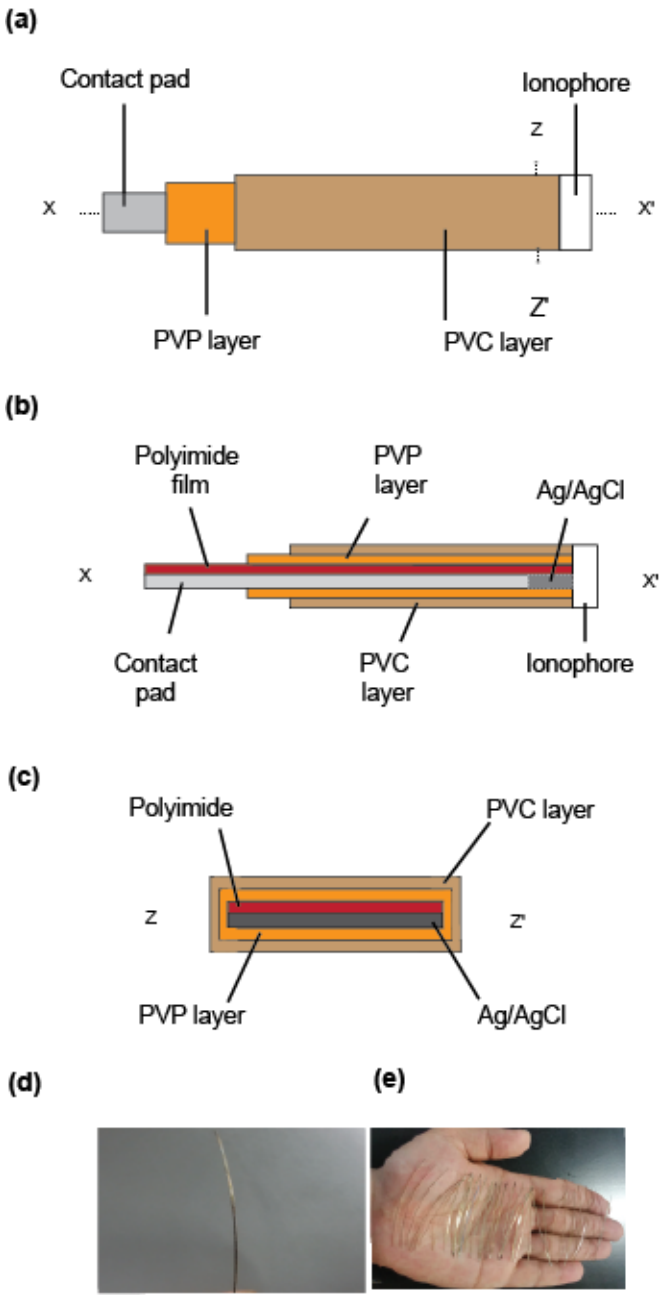

Fig. 3.2 Structure of the type-I ion-selective electrode. (a) A top view. (b) Cross section along the x-x'. (c) Cross section along z-z' direction. (d) Single electrode, and e) Multiple electrodes on the palm of the hand.

various step involved for the fabrication of the type-I ISE and RE are shown in Fig. 3.2.

Depending on the experiment, the type-II ISE and RE were fabricated. The structure of the type-II ISE and RE are shown in Fig. 3.3. The type-II ISE is constructed with a syringe needle (inner diameter: 0.9 mm), electrolyte solution, an Ag/AgCl electrode, and an ion-selective membrane. To form the ion-selective membrane, the syringe needle was cleaned with 99.99% ethanol for 10 min using a sonicator. Next, the syringe needle was dried on a hotplate for 20 min at 120 ^{o}C. The sharp end of the syringe needle was immersed in an ionophore solution to form the ion-selective membrane.

Next, the Ag/AgCl electrode and internal solution (0.1 M NaCl for the Na^{+} ion-selective electrode, and 0.1 M KCl for the type-II K^{+} ion-selective electrode) were introduced into the syringe needle to complete the ISEs. To fabricate the type-II RE, a similar procedure was followed. Here, a 3.0 M KCl solution was used instead of a 100 mM NaCl or KCl as an electrolyte solution. Also, the ion-selective membrane of the type-II ISEs was replaced with a poly(HEMA) liquid junction. To complete the RE, internal solution and Ag/AgCl electrode was incorporated in the syringe needle.

Fig. 3.4 shows how the electrolyte solution was introduced within the needle chamber. Briefly the electrolyte solution has taken into the conical centrifuge-tube. The Ag/AgCl electrode was incorporated in the syringe needle. Then, the syringe needle with the electrode was vertically inserted in the centrifuge tube. Next, the tube with electrode was placed introduced to the vacuum chamber and was removed the bubble by using vacuuming process. Therefore, the electrolyte solution was introduced within the needle chamber. Sometimes, these steps were followed two or three times depending on the requirements, but maximum cases one time was followed.

A polyimide sheet was used as substrate. Dimensions of the polyimide sheet was 80 mm × 60 mm. The surface of the sheet was made rough using the sand blaster. The sonicator was used to clean the sandblasted sheet. The sonication was done three times and fresh acetone was used every time for cleaning. Next, the electrodes were formed by a thin-film process. A 600-nm-thick silver layer was sputter-deposited on the polyimide base layer. A positive resist was used to cover the silver layer. Next the polyimide string with the silver was cut using dicing machine to form the multiple number of the polyimide strings. Finally, a fresh acetone solution was used to remove the positive resist from the polyimide strings.

The active area of the silver was protected by using a positive resist. During the protection, the two ends of the silver were exposed. One exposed end (0.8 cm) was used for growing the AgCl electrode, and other end was used for making the contact pad. The AgCl was grown in 0.8 cm silver

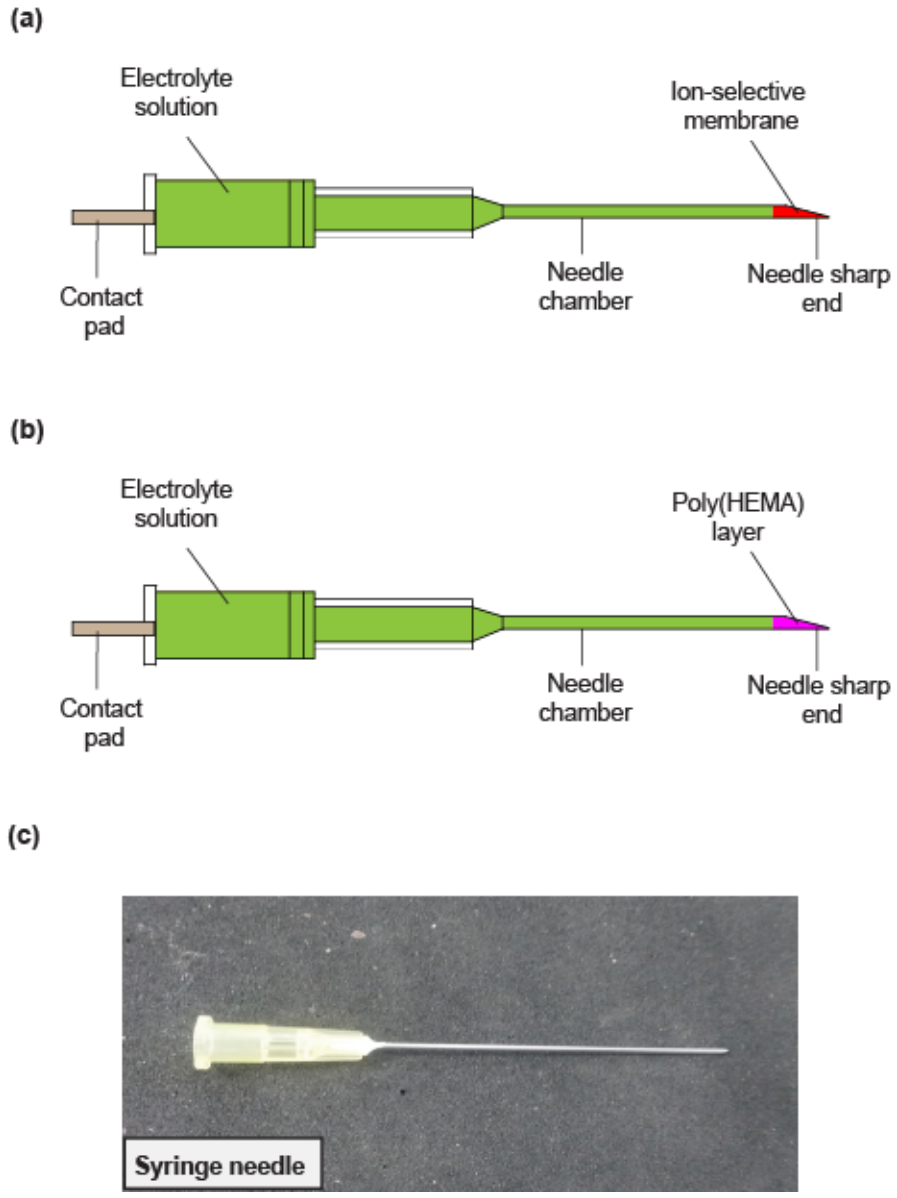

Fig. 3.3 The structure of the type-II ion-selective electrode and RE. (a) The structure of the type-II ion-selective electrode. The ion-selective membrane was formed at the sharp end of the needle. (d) The structure of the type-II RE. The end of the syringe needle was filled with poly(HEMA) solution as liquid junction. (c) A syringe needle (innner diameter: 0.9 mm).

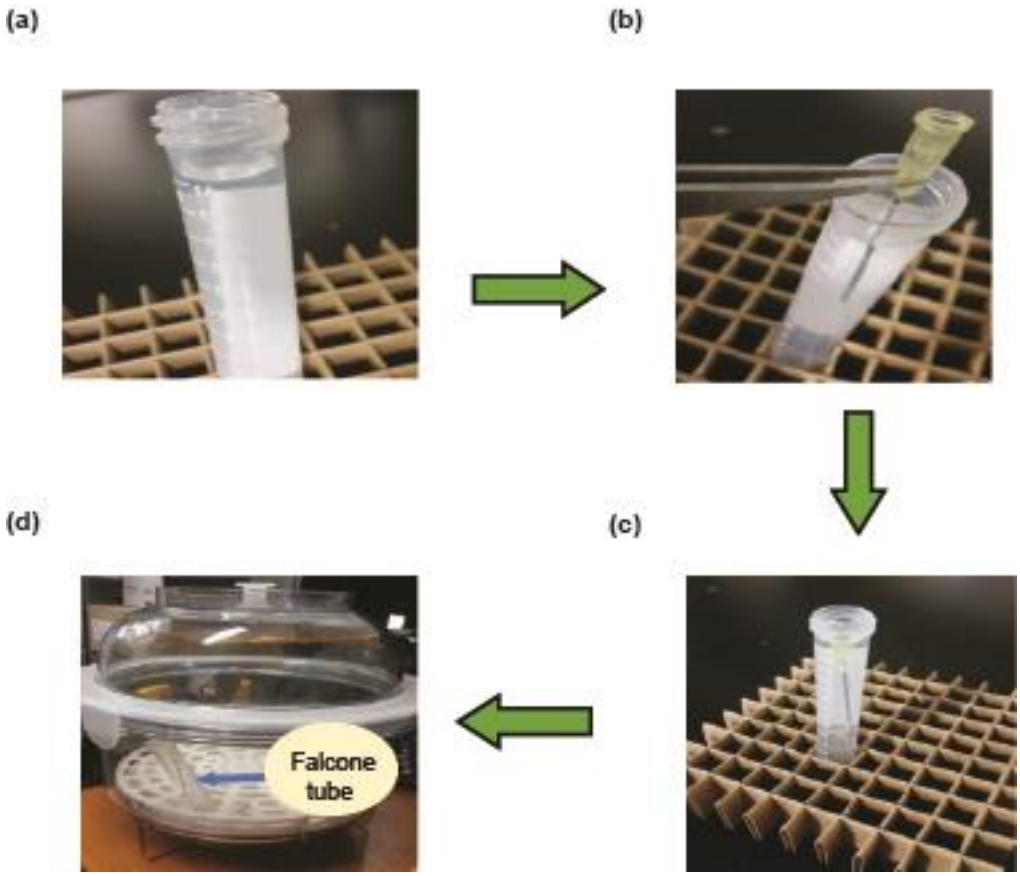

Fig. 3.4 The process of the introduction of the internal solution within the chamber of the syringe needle. (a) The electrolyte solution in the centrifuge tube. (b) Needle inserted vertically in the solution of the centrifuge tube. (c) Needle in the solution. (d) Centrifuge tube with needle in the vaccum chamber.

layer by applying a constant current (50 nA) for 10 min using a galvanostat (HA-151, Hokuto Denko, Japan) [26].

For the Na^+ ion-selective membrane, crown ether is a representative ionophore [5]. To form the membrane, 101 mg of PVC powder was dissolved in 7.6×10^3 µL of tetrahydrofuran (THF). Then, 200 µL of NPOE, 10 mg of bis(12-crown-4), and 6 mg of sodium tetraphenylborate were added. The mixture was thoroughly stirred to mix completely. Then, the end of the type-I ISEs or the sharp end of the syringe needle was immersed in the solution to form the membrane. The ISEs were stored in a plastic box with cover at room temperature for at least 24 h prior to the experiments.

For the K^+ ion-selective membrane, 5 mg of ligand (valinomycin), 1 mg of lipophilic additive (KTpClPB), 134 mg plasticizer (DOS), and 60 mg of PVC were mixed together [3-4]. To form the membrane, the mixer was dissolved in 2.5×10^3 µL tetrahydrofuran (THF) solution. The mixture was thoroughly stirred to mix completely. Then the end of the type-I ISEs or the sharp end of the syringe needle was immersed in the solution to form the membrane. The ISEs were stored in a plastic box with a cover at room temperature for at least 24 h.

To prepare the liquid junction for the type-I and type-II RE, a 0.05M poly(HEMA) powder was dissolved in ethanol as solvent. The solution was thoroughly stirred to mix properly. The type-I RE electrode end and the sharp end of the syringe needle were dipped in the poly (HEMA) solution to form the liquid junction. The liquid junction was inserted five times in poly(HEMA) solution and was removed immidiately. Finally, the liquid junction was formed after drying for 24 h. To complete ISEs and RE devices, a 0.1 M NaCl for the Na^+ ion-selective electrode (type-I and type-II), 0.1 M KCl solution for the K^+ ion-selective electrode (type-I and type-II), and 3 M KCl solution for the type-I and type-II RE were used as electrolyte solution.

3.2.3 Preparation of rice samples

The rice plant was grown in a greenhouse of the laboratory of crop sciences, Graduate school of Bio-agricultural Sciences, Nagoya University, Japan. The rice variety, Nipponbare, was used for the experiment. The rice plant was grown at control condition; high and low NaCl condition; and high and low KCl condition are shown in (Fig. 3.5).

Type-I ISEs were used to measure ion concentrations in dead plant parts. The experimental setup and the preparation of sample solution are shown in Fig. 3.6. Briefly, the rice plant parts were dried

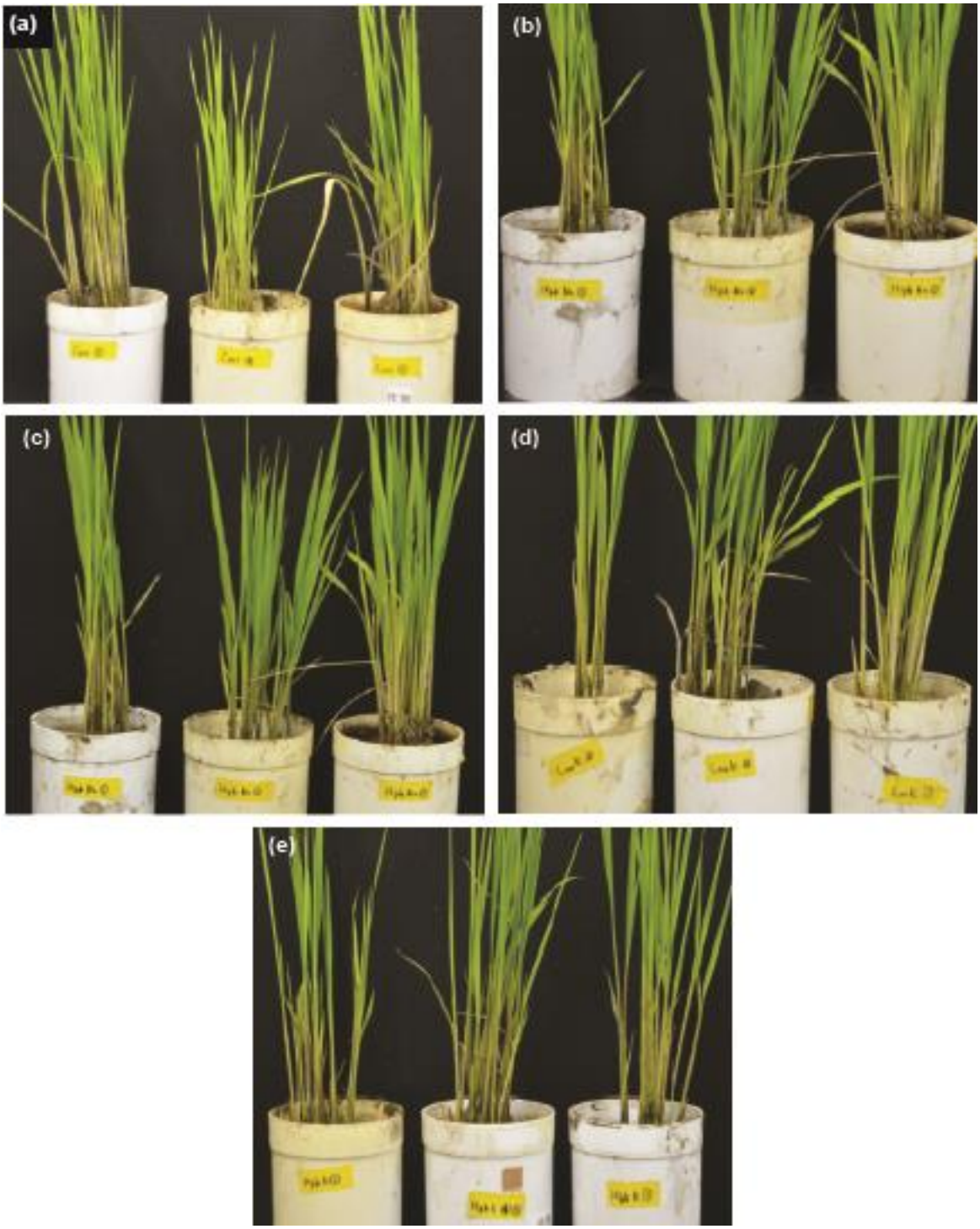

Fig. 3.5 The rice plant condition and experimental set up of type-II ISE with the live stem of the rice plant. (a) control, (b) low NaCl, (c) high NaCl, (d) low KCl, (e) high KCl treated rice plant.

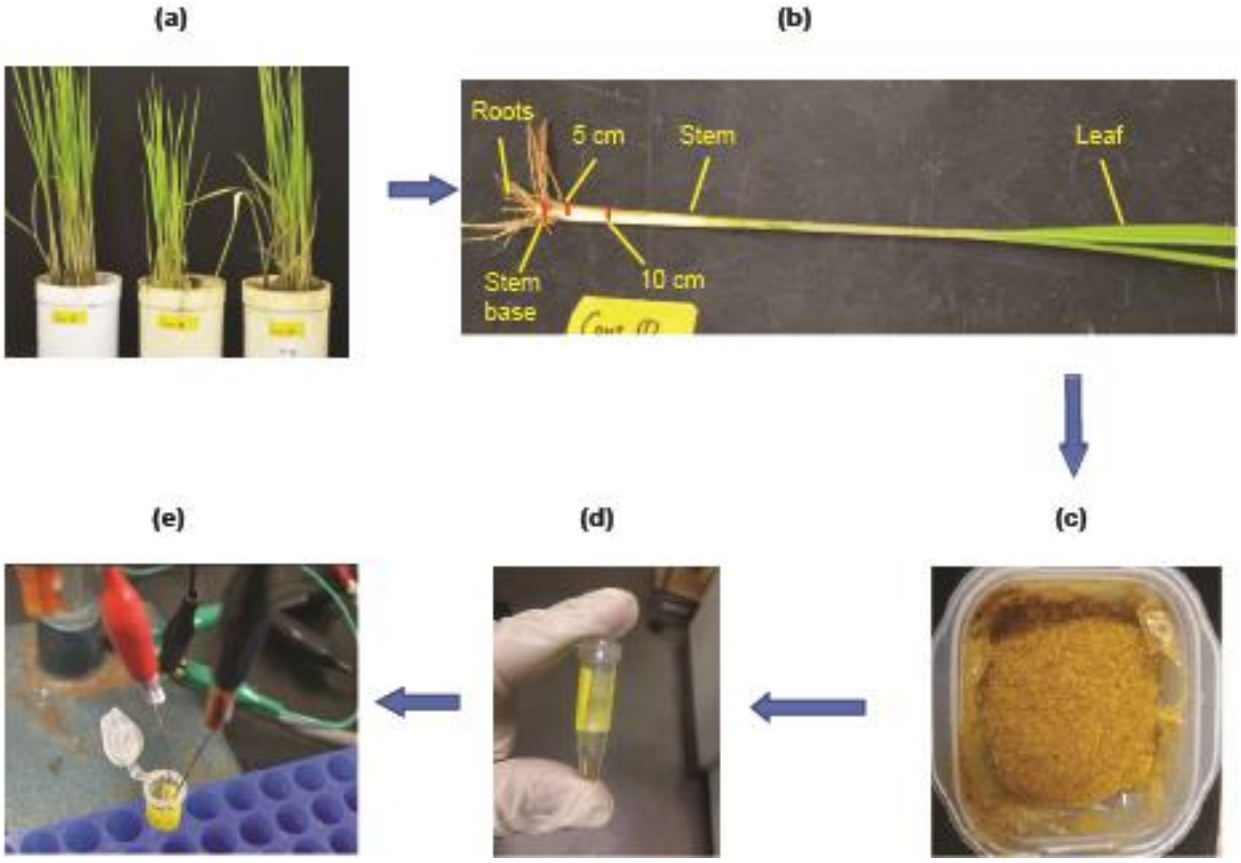

Fig. 3.6 The experimental set up of the type-I ISE. The collected rice plant was washed with the running tape water. The various part of the rice plant was dried with an oven at 120 ^{o}C for 24 h and ground to form the powder. The centrifuge of the sample was done at 15000 rpm for 1 minutes. The sensor was inserted into the sample solution for measuring the ion concentration.

on a hot plate at 120 ℃ for 48 h. The dried plant parts were crushed using a crusher to make powder. 10 ± 0.5 mg of the powder was taken in the Eppendorf tube. Milli-Q water was used to obtain 1 mL solution. The vortex mixer was used to mix the powder completely with water. Finally, the sample solution was centrifuged for 2 min at 15000 rpm to remove debris in the solution.

For the type-II ISEs, the Nipponbare rice plant was removed from the soil of the pot and immediately used for the measurement. The plant was cleaned with the running water and dried with tissue paper. The locations of measurement and the experimental set up are shown in Fig. 3.7. The stem base was the origin (0 cm) and the other locations were measured from there. The ISEs were inserted in the locations and the concentration of ions was measured one by one. The different rice plant was used for each experiment to measure the Na^+ and K^+ ions

The results obtained using the ISEs were compared with those obtained using an inductively coupled mass plasma spectrometry (ICP). The standard method was followed for the ICP sample preparation. Briefly, the dried plant part was heated on the hotplate at 120 ^oC for 48 h using a crusher to make the powder. A 20±0.2 mg of powder sample was taken into the Teflon tube. Nitric acid was added to the tube and the solution was kept overnight. The tube was heated in an oven for 24 h at 120°C to extract ions completely from the sample. Next, the tube was cooled down for 30 min or longer, 10 ml of the milli-Q water was added, and the solution was mixed well using a vortex mixer. Next, 4.95 µL of its supernatant was taken into the other tube and was stirred again using the vortex mixer. Finally, the sample solution was filtered with a filter paper (pore diameter: 0.45 µm).

3.2.4 Characterization of the devices

The response profile of the needle-type and syringe needle-type-ISEs was obtained with NaCl and KCl standard solutions, respectively. To characterize the performance of the ISEs, the ISE and the RE were immersed in a standard solution. After the potential was stabilized, the solution was discarded. The ion-selective membrane and the liquid-junction of the RE was cleaned with distilled water and then dried with a tissue paper. The next solution was then placed there. The same steps were repeated for all solutions.

Stability of the type-I and type-II RE was checked in a 3.0 M KCl solution in a beaker. Stability of the REs were tested in a concentrated KCl solution to check their performance under the extreme condition where the saline content may be high. Although the REs was tested in such extremity, the stability of the REs was not shown any significant change even after a exposing long time. A

(a)

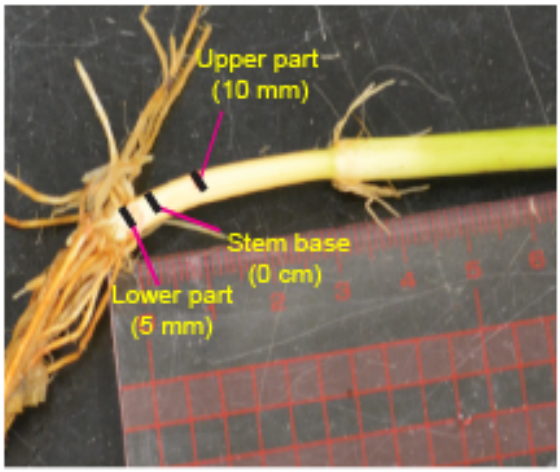

(b)

(c)

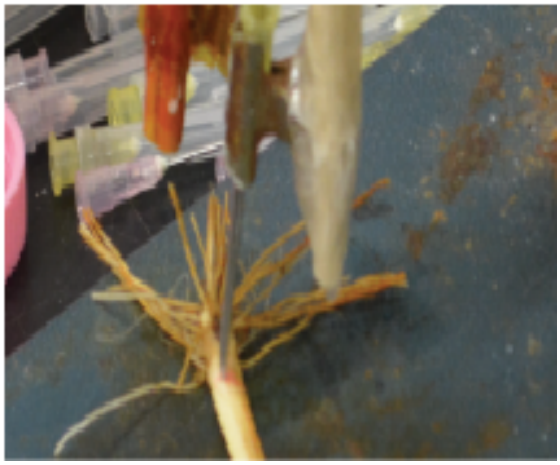

Fig. 3.7 The experimental set up of type-II ISE. (a) measured locations in the stem. (b) ISE inserted in the lower part of the stem (5 mm distance from the stem base). (c) the ISE inserted into the upper part (10 mm distant from the stem base).

commercial Ag/AgCl electrode (2060A, Horiba, Kyoto, Japan) was immersed in the solution. A 3.3 M KCl solution was used for the internal electrolyte solution of the commercial electrode. The potential of the type-I and type-II REs was measured with respect to the commercial electrode.

3.2.5 Measurement of Na^+ ion concentration in rice plants

The potential of the ISEs were measured with respect to the corresponding RE using an electrometer (AutoLab PGSTAT12, Eco Chemie, Utrecht, Netherland). For preconditioning, the Na^+ ion-selective electrode was immersed in a 100 mM NaCl and K^+ ion-selective electrode in the 100 mM KCl for 1 h. The ion-selective membrane and the liquid junction were cleaned with distilled water before starting the experiment. To use it on the other days, the ISEs were rinsed with water, gently dried with a tissue paper, and kept in a plastic box with a cover. Between the measurements with the same rice plant, the Na^+ ion-selective membrane was immersed in 100 mM NaCl solution, whereas K^+ ion-selective electrode in 100 mM KCl solution.

For the measurement, the type-I ISEs were used in the sample solution of the root, stem base, stem, green leaf and dead leaf, upper and lower part of the stem. Next, the type-II ISEs were inserted directly into the upper and lower part of the stem of the live rice plant. The rice plant was discarded every time after the measurement. Na^+ ion concentration was calculated based on the calibration plot obtained with NaCl standard solutions. The concentration was calculated using the calibration plot obtained with the standard solution. The internal solutions of ISE and RE for syringe needle-type (type-II) ion-selective electrodes and the REs were replenished with a fresh solution every time prior to the measurement. For the type-I ISEs and RE, the solid internal layer of the electrodes was wet by dipping them into the 0.1 M KCl and 3 M KCl for 5-10 minutes, respectively. The experiments were conducted at 25 °C.

3.3 Results and discussion

3.3.1 Performance of the ISEs

The stability of the type-I and type-II reference electrode was checked in a 3.0 M KCl solution. A commercial Ag/AgCl reference electrode (2060A, Horiba, Kyoto, Japan) was immersed there. A 3.3 M KCl solution was used for the internal solution of the commercial electrode. The potential settled at approximately 0 mV for the type-I and type-II reference electrodes, which are expected from the

Nernst equation. The potential was stable for at least 12 h for the type-I RE and 20 h for the type-II RE. It indicates, a reliable measurement can be conducted for a long time (Fig. 3.8). Fig. 3.9 shows the calibration plots of the needle type-I ion-selective electrodes. For the type-I and type-II Na^+ ion-selective electrodes, the potential was changed with the changes of the standard NaCl solution sequentially with an ISE. The potential was shifted in the positive direction with the increase in Na^+ ion concentration.

Fig. 3.9 (a-b) shows the relationship between the measured potential and the Na^+ ion concentration of the needle-type Na^+ ion-selective electrode with respect to the commercial and the poly(HEMA) based reference electrode. As anticipated from the Nernst equation, a linear relationship was observed for both cases in the examined concentration range. The slopes of the plots for the type-I Na^+ ion-selective electrode with respect to the commercial and poly(HEMA) based RE were +50.0 and +52.9 mV/decade, respectively. The slopes of the plots for the type-II Na^+ ion-selective electrode with respect to the commercial and poly(HEMA) based RE were 56.9 and +57.8 mV/decade, respectively.

Similarly, the type-I and type-II K^+ ion-selective electrode were characterized with the standard solution of the KCl with respect to the commercial Ag/AgCl electrode and the poly(HEMA) based reference electrode. The potential was shifted in the positive direction with the increase in K^+ ion concentration. The slopes of the calibration plots for the type-I Na^+ ion-selective electrode with respect to the commercial and poly(HEMA) based RE are +55.9 and +50.9 mV/decade, respectively (Fig 3.9 (c)). The slopes of the plots for the type-II Na^+ ion-selective electrode with respect to the commercial and poly(HEMA) based RE are +50.4 and +51.0 mV/decade, respectively (Fig 3.9 (d)). The values obtained with the two needle-types Na^+ and K^+ ion-selective electrodes were close to Nernst slope, demonstrating that the needle-type ISEs along with the RE can be used for the measurement. The experiment was conducted at 25 ^oC.

3.3.2 Measurement of Na^+ ion concentration in rice plants

The measurement of the ion concentration is very much important to know the growth, height, weight, seed yield, etc. The ion has both positive and negative effect on the plant. The excess level of the salt is harmful for the plant. The Nipponbare rice variety was used for the experiment. We measured the ion concentration in the rice plant using both type-I and type-II ISEs. Measurement of the ion concentration with the type-I ISEs are shown in Fig. 3.10. Na^+ ion concentration was found higher in the roots than in the shoots (Fig.3.10 (a)). Also, Na^+ ion concentration was found higher at the lower part of the stem and found lower at upper part (Fig. 3.10 (b)). Alternatively, K^+ ion

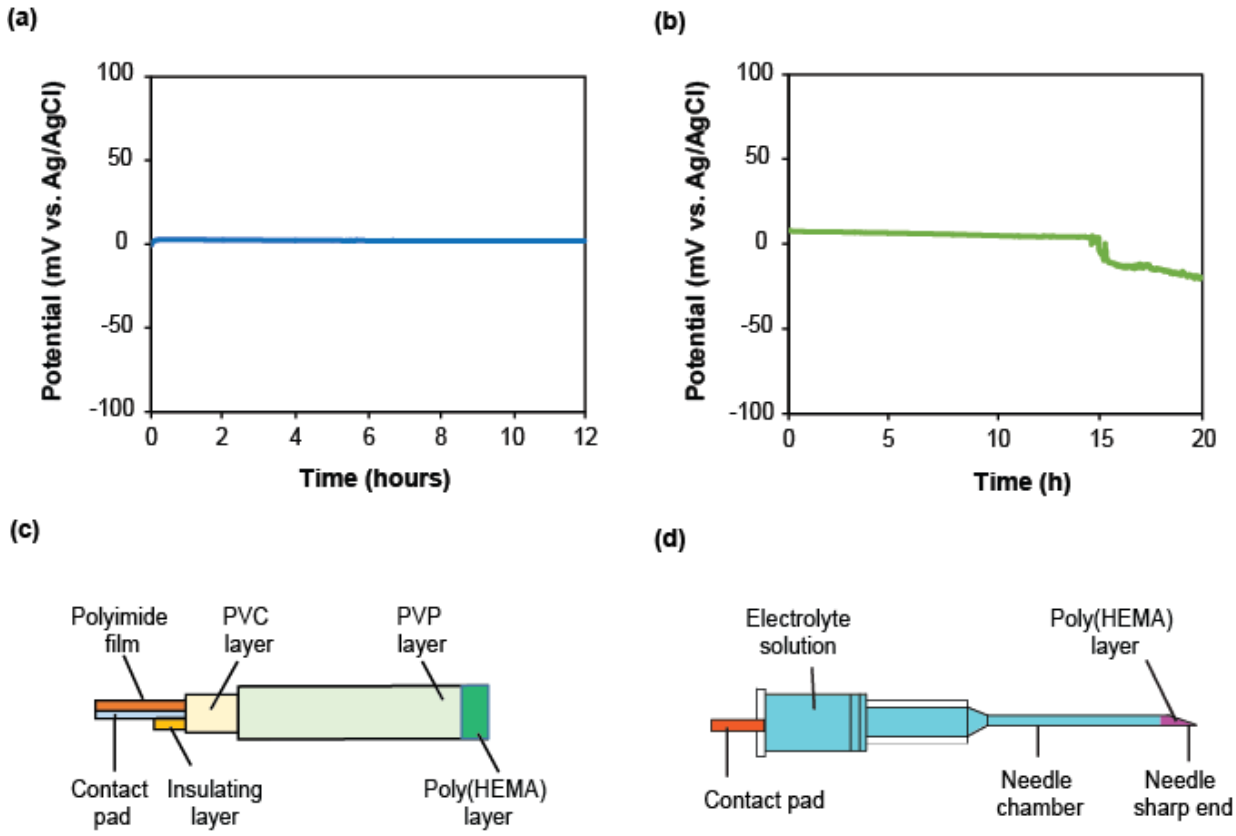

Fig. 3.8 Checking the stability of the needle-type reference electrode in a 3 M KCl solution with respect to the commercial reference electrode. (a) The stability of the type-I poly(HEMA) reference electrode. (b) Checking the stability of the type-II poly(HEMA) RE. (c) Structure of the type-I poly(HEMA) RE. (d) The structure of the type-II poly(HEMA) RE.

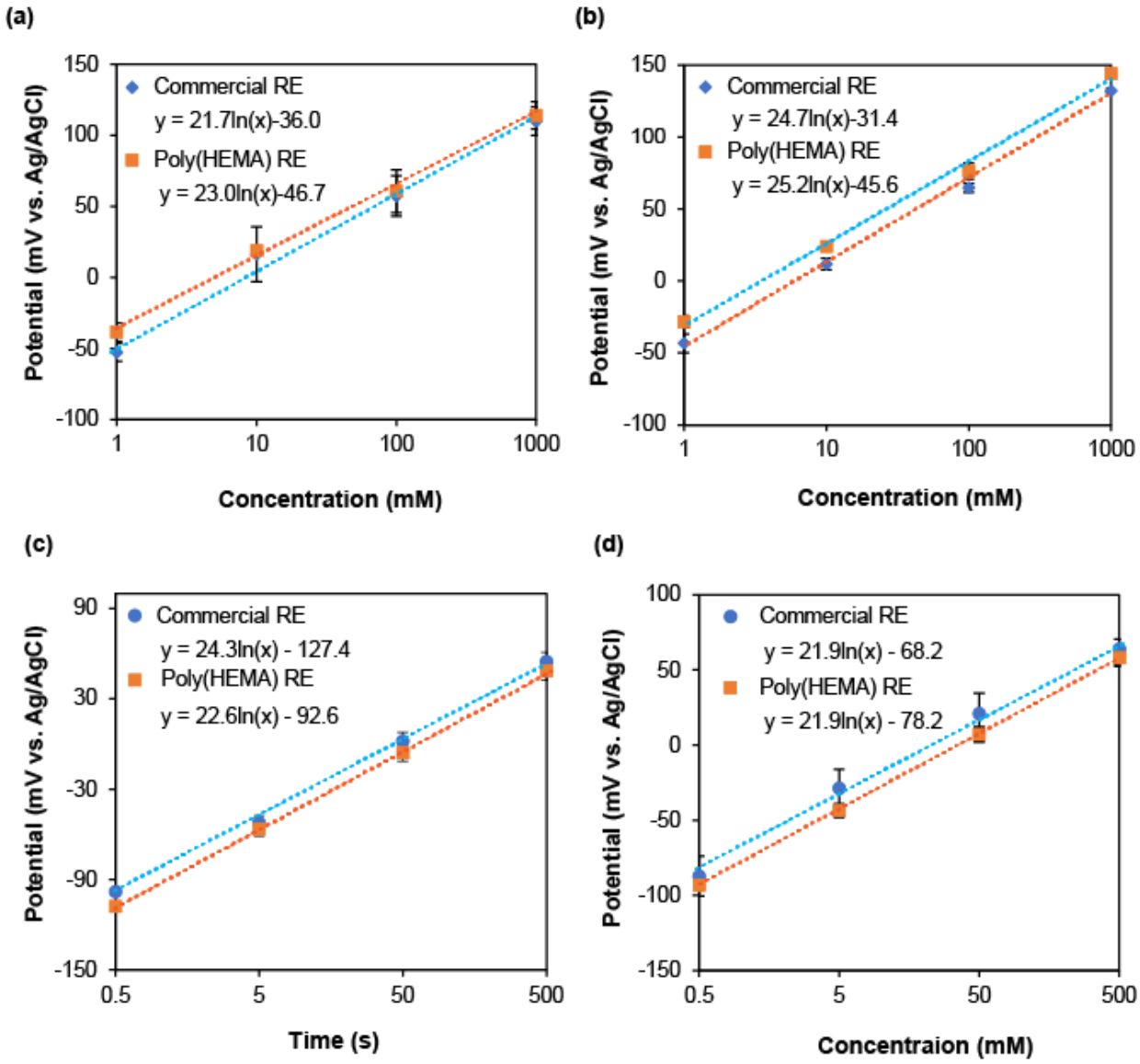

Fig. 3.9 The characterization of the ion-selective electrodes. The calibration plot of the (a) Type-I and (b) the type-II Na^+ ion-selective electrode. The calibration plot of the (c) type-I and (d) the type-II K^+ ion-selective electrode.

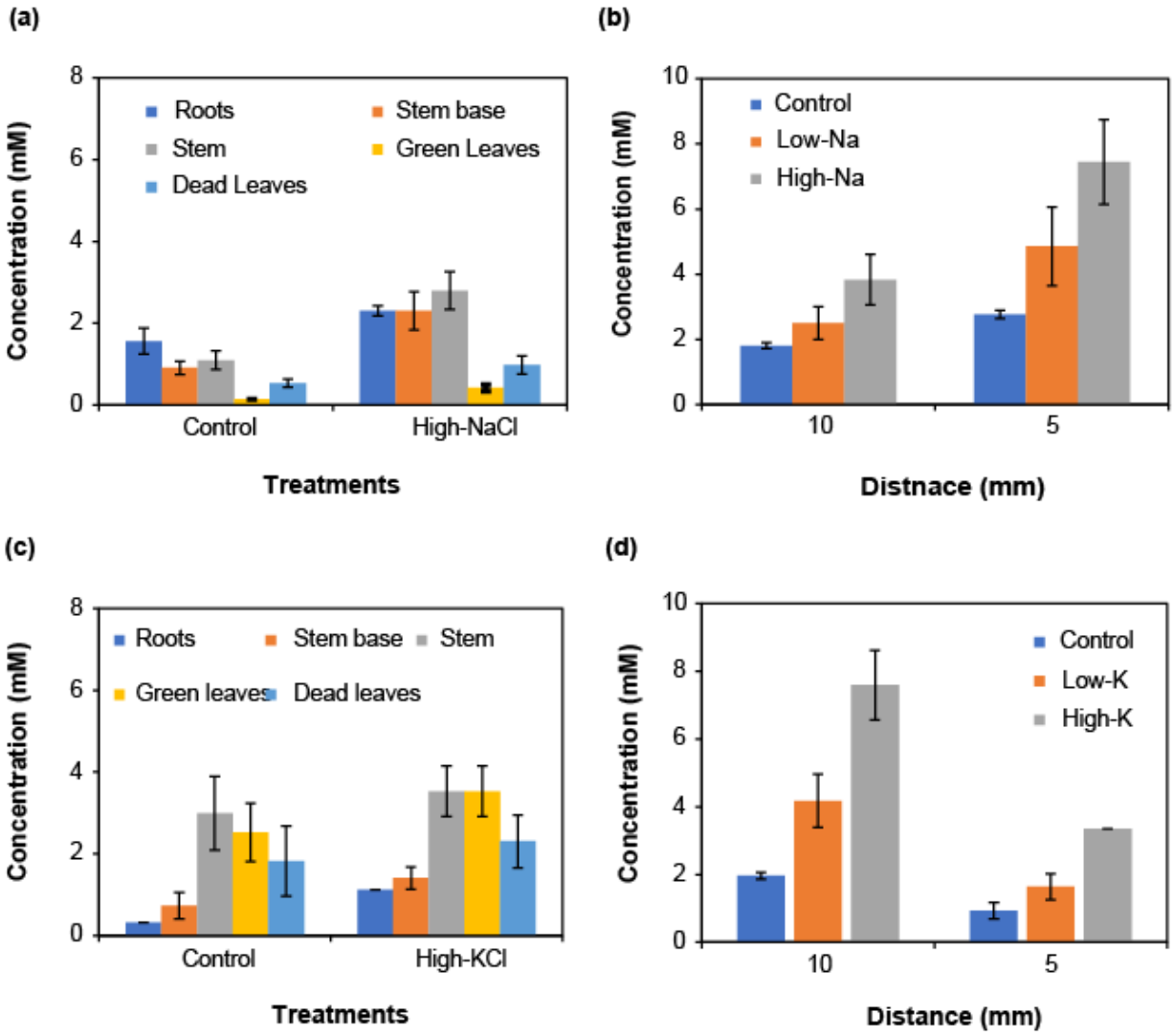

Fig. 3.10 Measurement of the ion differences in the various parts of the plant using type-I ISE. (a) The measured Na^+ ion concentration at various part of the rice plant. (b) The Na^+ ion obtained at the lower and upper part of the stem. (c) The K^+ ion variation obtained with the type-I ion-selective electrode in the samples. (d) The K^+ ion measurement at the upper and lower part of the stem.

concentration was found higher in the shoot than the roots (Fig.3.10 (c)). The upper part of the stem has shown higher K^+ ion concentration than the lower part (Fig.3.10 (d)). Both the Na^+ and K^+ ion concentration was increased with the increases of the salt concentration at the root of the rice plant. These results are agreed with the results obtained by [6].

The obtained results with the type-I Na^+ and K^+ ion-selective electrodes were compared with the inductive coupled plasma atomic emission spectrophotometry (ICP-AES) method (Table 3.1). ISEs has shown similar tendencies like ICP method. The concentration measured with both method was found similarities. But some cases the differences were observed between two methods. Preparation of the sample preparations and the ages of the plant are the probable causes for this variation.

Depending on the measurement, the type-II ISEs were fabricated. ISEs were inserted into a live rice plants. A two-week old seedling Nipponbare rice plant was used for the experiment. The measured ion concentration is shown in Fig. 3.11. The ion was measured at upper part and the lower part of the stem. The Na^+ ion concentration was found higher in the lower part than the upper part. Alternatively, the K^+ ion concentration was observed lower in the lower part than the upper part. In both cases of ion, the concentration was increased with the increases of the salt concentration at the root system. The tendency of the measured ion concentration has shown similarities with the type-I ISE. These results indicated that the type-II ion-selective electrode could be used for the direct measurement of the ions in the live rice plants.

3.4 Summary and conclusions

The needle-type (type-I) and syringe needle-type (type-II) ISEs were fabricated. The electrodes can be very inexpensive due to the use of polyimide as a substrate and many electrodes produce through single batch-fabrication process. Depending on the experimental purpose, the type-I ISE used in the sample solution and the type-II ISE was used in the live plant for direct measurement of the ion. Therefore, the syringe needle-type ISE can be inserted directly into the stem of the rice plant or other hard samples. The type-II ISE is applicable to the direct measurement of Na^+ and K^+ ion concentration without any pretreatment. Thin-film Ag/AgCl electrodes were used for the fabrication of the ISE and RE. For making the RE we used poly(HEMA) to make the liquid junction. The stability of the liquid junction. The stability of the type-I and type-II RE were examined. The electrodes actually provided stable potentials expected as an Ag/AgCl electrode for a sufficiently long time needed for measurements. The ion concentration measured using the type-I ISEs agreed well with

Table 3.1. Comparative study of the type-I Na^+ ion-selective electrode and K^+ ion-selective electrode with the ICP-AES method. The blue color for the type-I Na^+ ion-selective electrode and the red color for the type-I K^+ ion-selective electrode.

Measured parts	NaCl salt treatment	ICP-AES $_{x}10^4$(mg/Kg)	Type-I Na-ISE $_{x}10^4$(mg/kg)	KCl salt treatment	ICP-AES $_{x}10^5$(mg/kg)	Type-I K-ISE $_{x}10^5$(mg/kg)
Roots	Control	0.30	0.20	Control	0.02	0.03
	High-Na	0.43	0.53	High-K	0.02	0.05
Stem base (fresh)	Control	0.04	0.03	Control	0.08	0.09
	High-Na	0.05	0.08	High-K	0.12	0.12
Stem	Control	0.42	0.24	Control	0.10	0.11
	High-Na	0.42	0.62	High-K	0.11	0.14
Green leaves	Control	0.07	0.01	Control	0.07	0.06
	High-Na	0.09	0.22	High-K	0.91	0.82
Dead leaves	Control	0.25	0.36	Control	0.16	0.13
	High-Na	0.32	0.53	High-K	0.13	0.44

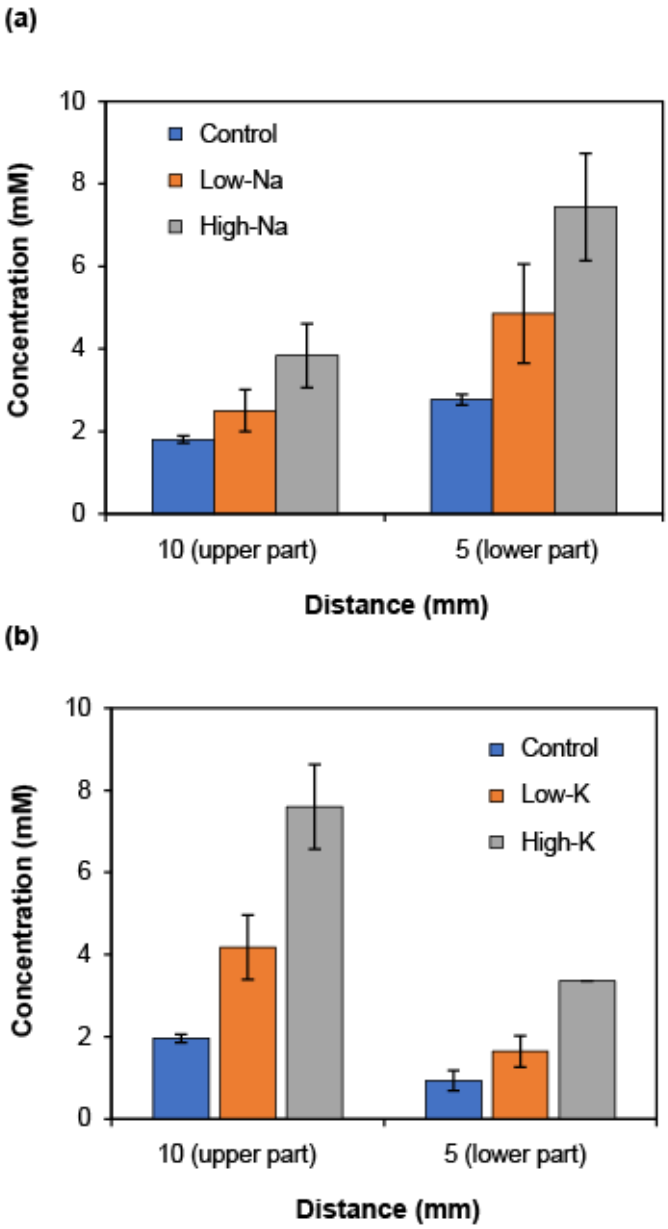

Fig. 3.11 The measurement of the ions in the live plant using type-II ISE. (a) The measurement of Na^+ ion with type-II Na^+ ion-selective electrode. (b) The K^+ ion concentration with the type-II K^+ ion-selective electrode.

those obtained using the conventional ICPs method. On the basis of this technique, ion-sensing devices for other ions can also be realized. The developed ISEs will be a useful tool for the efficient screening of salt-tolerant plant.

References

1. V.P.Y. Gadzekpo, J.M. Hungerford, A.M. Kadry, Y.A. Ibrahim, and G. D. Christian: Anal. Chem. **57** (1985) 493.
2. E. Metzger, R. Dohner, W. Simon, D.J. Vonderschmitt, K.Gautschi: Anal. Chem. 59 (1987) 1600.
3. S. J. Birrell, and J. W. Hummel: Trans. ASAE. **43** (2000) 206.
4. M.Knoll, K. Cammann, C. Dumschat, M. Borchardt, and G. Hogg: Sensors and Actuators B. **20** (1994) 5.
5. P. Bühlmann, E. Pretsch, and E. Bakker: Chem. Rev. **98** (1998) 1593.
6. V. Varaporn, N. Malee, K.Lily Srisom S. J.Ian: Theoretical and Experimental Plant Physiology. 25 (2013) 115.

Chapter 4: Easily Batch-Fabricated Clark-Type Oxygen Electrodes for Plant Researches

4.1 Introduction

Dissolved oxygen is one of the most important parameters for understanding of the mechanism of the nitrogen fixation in rice plants. To increase the production of rice without application of chemical fertilizers, the nitrogen-fixing mechanism in rice plant needs to be improved urgently. But, the nitrogen-fixing mechanism is completely depending on the nitrogen-fixing bacteria. The nitrogen-fixing bacteria can survive in the soil of the root system in presence of the oxygen. Oxygen deficiency is causing the death of the bacteria. Therefore, the information of dissolved oxygen concentration in the rice root and its parts at various points of the technological line is essential for developing a sustainable agriculture system.

The sample analysis method (Winkler method) has used to measure the dissolve oxygen level in the laboratory. But it has required high resolution of data to measure the compounds. Also, it is costly process, time consuming, and requires technical operator. Moreover, the accuracy, reliability and complexity of the method is very less. Now a day one of the main encounters is the advance of methods to accomplish the rapid both laboratory and filed based analyses. These methods must be sensitive and accurate, and able to determine various substances with different properties in ‘‘real-life’’ samples.

To this end, the Clark-type oxygen might be a good choice. Because, it is inexpensive, high selectivity, high sensitivity, and rapid, which are able to use in the real samples. Also, the oxygen-electrode made with immobilization of organisms and enzymes have been used to analyze the various biological samples. Various tools have already been used to measure the dissolved oxygen level in biological samples. Among them, the Clark-type oxygen-electrode has been used in clinical analysis, fermentation monitoring, scientific research, food industry, and development of biosensors [1].

Various miniature Clark-type oxygen-electrodes have been proposed based on CMOS (Complementary Metal Oxide Semiconductor) or MEMS (Micro Electro-Mechanical Systems) techniques over the last two decades [2–12]. Although some of them have been commercialized, they are extremely expensive. Also, many of them were not necessarily suited for the application to plant

researches. To solve these problems, we fabricated simple cost-effective oxygen electrodes particularly aiming for measurement of the oxygen in the rice plant.

4.2 Experimental section

4.2.1 Reagents and materials

Materials and reagent used for the fabrication and characterization of the devices were purchased from the following commercial sources: a polyimide film (130 μm thick) from JMT Corporation (Osaka, Japan); a silicone adhesive (KE42) from Shin-Etsu Chemical (Tokyo, Japan); a positive photoresist (S-1818G) from Dow Chemical (Midland, USA); polyvinyl chloride (PVC) powder, tetrahydrofuran (THF), polyvinylpyrrolidone (PVP) and the other reagents from Wako Pure Chemical Industries (Osaka, Japan). Syringe needles (1.2 mm in inner diameter) were purchased from Terumo (Tokyo, Japan). All solution was prepared with Milli-Q water (Millipore, Tokyo, Japan).

4.2.2 Fabrication of the needle-type oxygen electrode

The structure of the needle-type (type-I) oxygen electrode is shown in Fig. 4.1. It consists of a cathode, an anode, an oxygen-permeable membrane, an electrolyte layer, and a PVC coating (reservoir) layer. The electrode was prepared by sputtering and dicing process. For this purpose, both side of a polyimide substrate were sandblasted using a sandblaster for 20-30 s to make the substrate surface rough and improve the adhesion of metal films to the substrate. Next, the substrate was cleaned with distilled water and acetone using a magnetic stirrer. The substrate was further cleaned three times in acetone using a sonicator for 15 min in total (5 min × 5 min × 5 min). Fresh acetone was used each time.

Platinum and silver layers were sputter-deposited on both sides of the polyimide substrate (80 mm × 65 mm) to make the cathode and anode, respectively. The thickness of the platinum and silver layers were 150 nm and 560 nm, respectively. One end of the electrodes was used as contact pads and the other end (1 mm) was used as the sensitive area. To this end, the active areas of the electrodes were delineated with a polyimide layer. To form the layer, the polyimide prepolymer solution was spin-coated and was baked for 30 min at 80 °C. Next, a positive photoresist was spin-coated and was baked for 30 min at 80 °C.

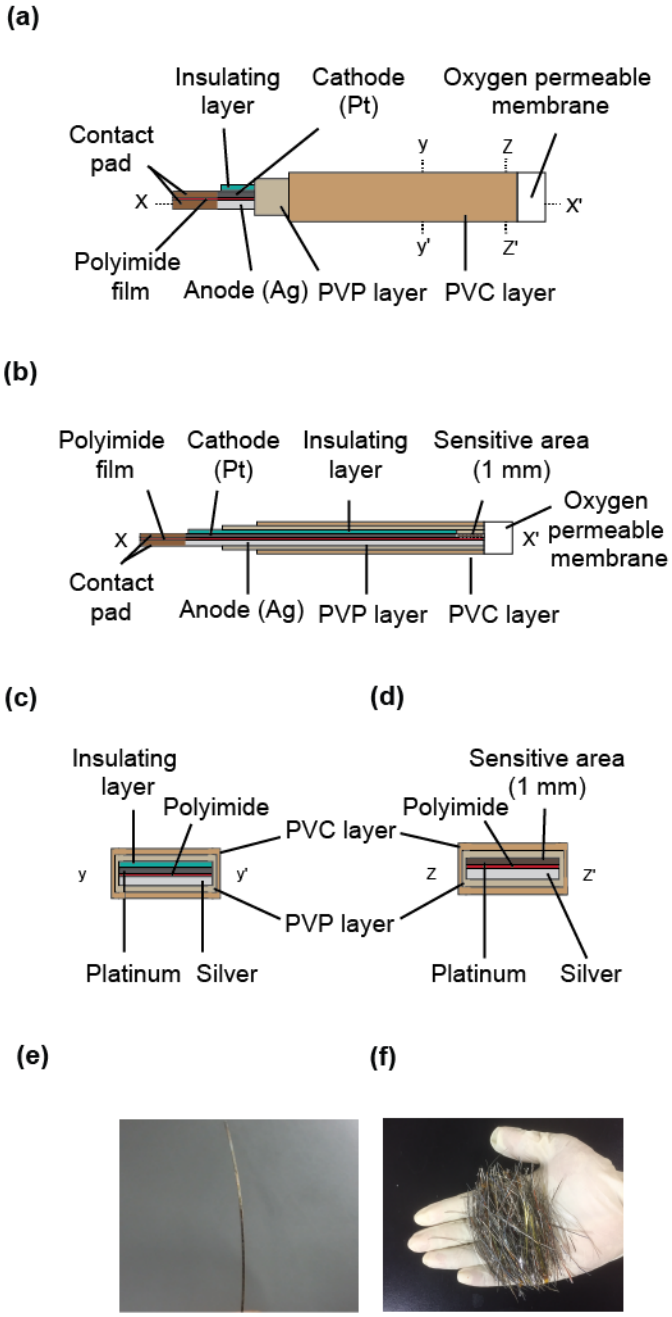

Fig. 4.1 The structure of the type-I oxygen electrodes. (a) A top view. (b) Cross section along x-x' direction. (c) Cross section along y-y' direction. (d) Cross section along z-z' direction. (e) Single electrode. (f) Multiple electrode on the palm of the hand.

For patterning of 1 mm sensitive area, a positive photoresist pattern was formed on the polyimide film using a mask aligner. The photoresist was developed in a developer solution for 1 min. After that, the substrate was rinsed with distilled water for 1 min and in ethanol for 2 min. Finally, the substrate was cured at 150 ^{o}C for 15 min, at 200 ^{o}C for 15 min, and at 280 ^{o}C for 30 min. The polyimide substrate with electrodes was cut into thin strings using a dicing machine. The length and pitch of the electrode was obtained as 65 mm and 0.5 mm, respectively.

The fabrication process of the type-I oxygen electrode is shown in Fig. 4.2. An electrolyte layer was then coated on the electrodes. To this end, a 75% PVP solution was prepared by dissolving the PVP powder in a 0.1 M KCl solution. The electrode end was immersed in the PVP solution and was removed from the solution immediately is shown in the Fig. 2 (b). The dry PVP layer was obtained after drying for 30 min (Fig. 4.2 (c)). THF was used as a solvent for making a 66% PVC solution. The polyimide string with the dry electrolyte layer was immersed in the PVC solution (Fig. 4.2 (d)). The PVC-coated electrodes were dried for 10 min to form the reservoir for the electrolyte layer. (Fig. 4.2 (e)). After forming the electrolyte chamber, the end of the Ag/AgCl electrode was cut using a scissor (Fig. 4.2 (f)). The cut end was inserted in the silicone adhesive (Fig. 4.2 (g)) to form the oxygen-permeable membrane at the cut end. The oxygen-permeable membrane was formed after drying for 24 h (Fig. 4.2 (h)).

When an appropriate potential is applied to the working electrode (cathode) with respect to the reference electrode (anode), oxygen is reduced on the cathode, generated current changes in proportion to dissolved oxygen concentration under the diffusion limiting condition.

In the oxygen electrode, the state of AgCl in the Ag/AgCl anode influences the stability and determines the lifespan. To form the AgCl layer during the fabrication process is not efficient, as the layer is easily damaged by the dissolution of AgCl accompanying the formation of silver complexes [21]. Therefore, AgCl was grown during the operation of the oxygen electrode.

Depending on the experiment, the oxygen electrode needs to be directly inserted into a plant. For this purpose, another type of oxygen electrode that employs a syringe needle (type-II) was fabricated. The structure of the syringe needle-type (type-II) oxygen electrode is shown in Fig. 4.3. The type-II oxygen electrode is constructed with a syringe needle (inner diameter: 1.2 mm), electrolyte solution, an anode, cathode and oxygen-permeable membrane. The polyimide string with the cathode and anode used in the type-I oxygen electrode that was also used fabricating the type-II oxygen electrode. An electrolyte layer and the PVC coating formed in the case of the type-I device were not formed

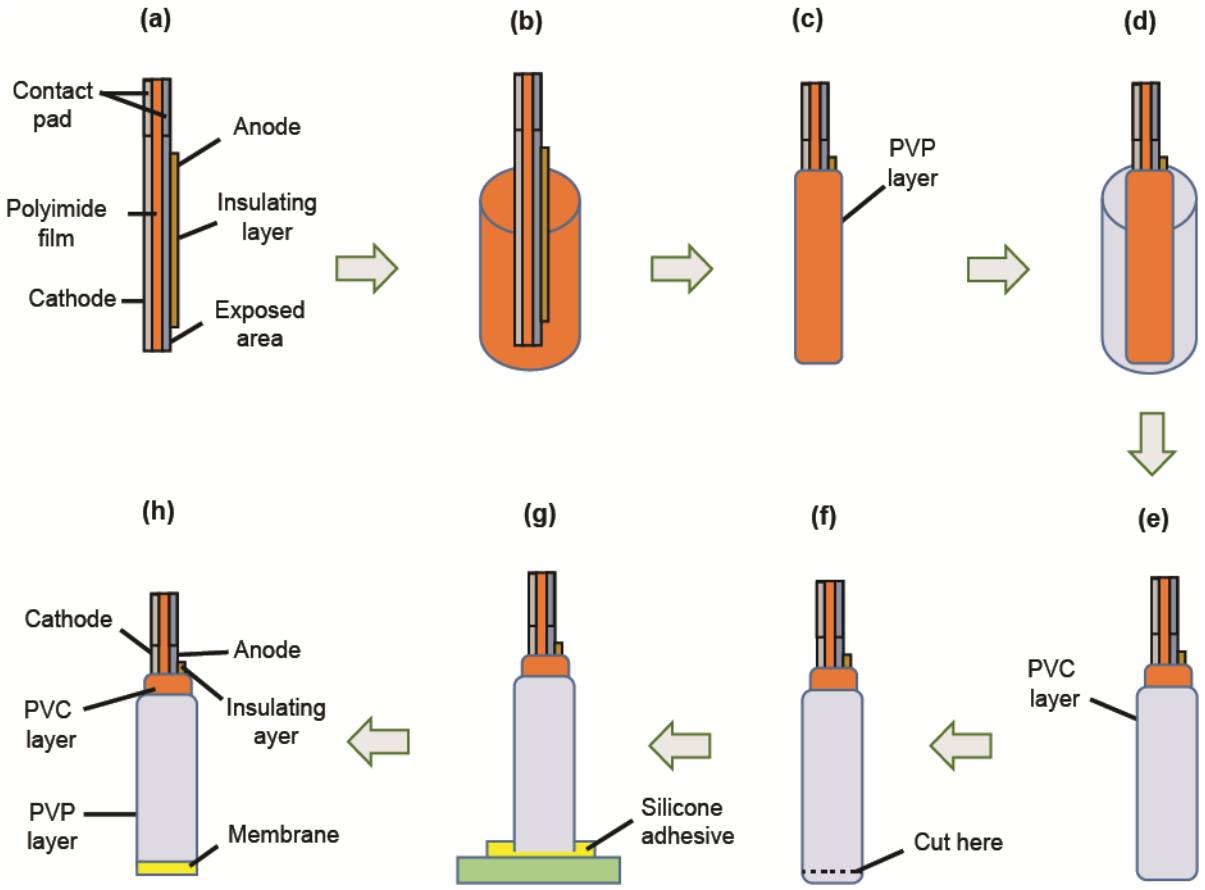

Fig. 4.2. Fabrication of the needle type (type-I) oxygen electrode. The preparation of electrolyte layer, reservoir and oxygen permeable membrane.

(a)

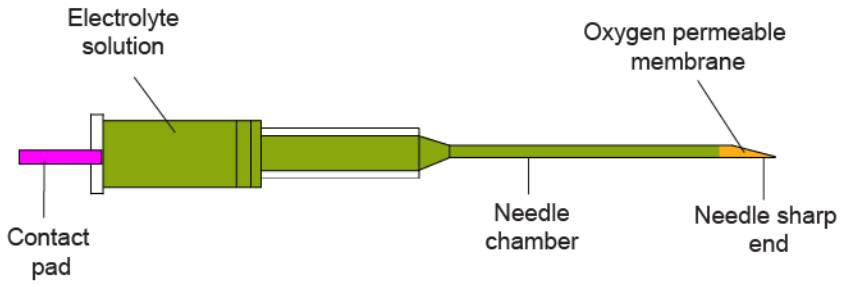

(b)

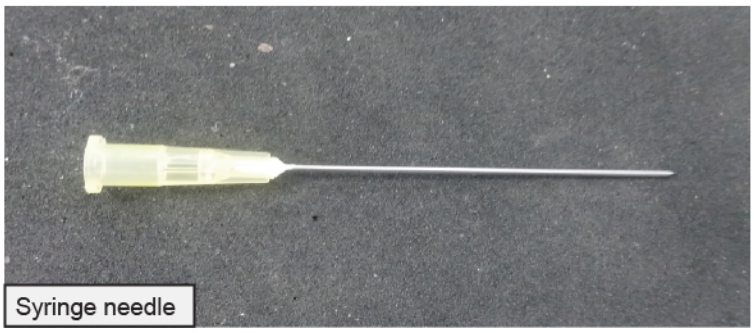

Fig. 4.3. The structure of the type-II oxygen electrode. (a) The type-I oxygen electrode. (b) A syringe needle (inner diameter: 1.2 mm).

here. As in the case of the previous device, a 0.1 M KCl solution used for making the electrolyte layer, which was also used as an electrolyte solution for the type-II oxygen electrode.

To form the oxygen-permeable membrane, the syringe needle was cleaned with 99.99% ethanol for 10 min using a sonicator. Next, the syringe needle was dried on a hotplate for 20 min at 120 ^{o}C. The sharp end of the syringe needle was inserted in a silicone adhesive to form the oxygen-permeable membrane. The membrane was used for the experiment after drying it for 24 h. Next, polyimide electrode (cathode and anode) string and internal solution (0.1 M KCl) were incorporated in syringe needle. The electrodes were introduced within the needle chamber using forceps before doing the vacuuming. A 0.1 M KCl solution was introduced within the needle chamber by using a vacuum desiccator. The vacuum process was also effective to remove bubbles from the chamber.

4.2.3 Electrical connection to the electrodes

The connection between alligator clip and the electrodes are shown in Fig. 4.4. The electrodes were connected to a potentiostat for amperometric measurement (Autolab PGSTAT12; Eco Chemie, Utrecht, Netherlands). One side of an alligator clip was insulated with polyimide tape, and the other side was wrapped with an aluminum foil. For the connection of clip to the electrodes, the aluminum foil insulated side was connected to the either anode or cathode. If the alligator clip is connected to the cathode and polyimide tape wrapped side connected to the anode, then it will act as a connector for the cathode. Similarly, while the aluminum foil insulated side of an alligator clip is connected to the anode and polyimide tape wrapped side connected to the cathode, then it will act as connector for the anode. Finally, the other end of an alligator clip was connected to the potentiostat.

4.2.4 Preparation of rice plant samples and RS1 bacterial medium

The rice plant was grown at a greenhouse of the laboratory of crop sciences, Graduate school of Bio-agricultural sciences, Nagoya University, Japan. The plant was grown in plastic pot (Fig. 4.5) A two-week old seedling plant stem and root were used for the measurement. First, dissolved oxygen concentration was measured in the bacterial medium. To observe the activity of the bacteria at different oxygen level, the two types of oxygen medium were prepared. For this purpose, the nitrogen-fixing bacteria (*Burkholderia vietnamiensis)* was isolated from the sweet potato and was grown at the bacterial medium. The bacteria were collected from sweet potato. Because, this

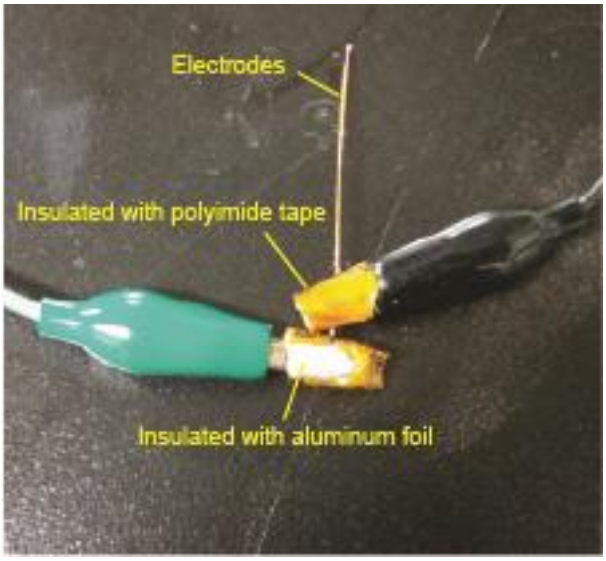

Fig. 4.4. The connection between alligator clips and electrodes.

Fig. 4.5. A Nipponbare rice plant and the **e**xperimental setup. (a) Control Nipponbare rice plant. (b) Control liquid medium (0% oxygen). (c) Semi-solid bacterial medium (21% O_2). (d) Insertion of the type-I oxygen electrode in the soil. (e) Measured location in the rice stem. (f) Type-II oxygen electrode inserted in the stem of the live rice plant.

bacterium can fix the atmospheric nitrogen to produce the nitrogen fertilizer for the sweet potato.

4.2.5 Characterization of the oxygen electrodes

Cyclic voltammograms of the bare platinum electrode was examined with an electrolyte solution (0.1 M KCl) in respect to the commercial Ag/AgCl reference electrode (2060A, Horiba) and a platinum auxiliary electrode. A 3.3 M KCl solution was used for the internal solution of the commercial Ag/AgCl reference electrode. The bare platinum electrode, platinum counter electrode and Ag/AgCl reference electrode were inserted into the solution.

For checking the stability of the electrode, the oxygen-permeable end of the electrode was immersed into the buffer solution saturated with air at 25 ºC. An approximately 1 cm length of the oxygen electrode was dipped into the solution. The solution was gently stirred using a magnetic stirrer. The response of the electrode was checked before and after the experiment.

4.2.6 Measurement of the oxygen level in the bacterial medium

Both the control (solution) and semi-solid (gel) bacterial medium are shown in Fig. 4.5 (a-b). The type-I oxygen electrode was inserted at 0 mm (surface), 1 mm, 2 mm, 3 mm and 4 mm depth of both medium. Next, the dissolved oxygen level was measured using the type-I oxygen electrode. The type-I oxygen electrode was also used for measuring the oxygen level in the soil of the rice root system to record the current change at various depths of the soil. On the other hand, the type-II oxygen electrode was inserted into the stem of the rice plant to observe the oxygen level at the different depths.

4.2.7 Measurement of the oxygen level in the stem of the live rice plant

The syringe needle-type oxygen electrode (type-II) was used for the measurement of the dissolved oxygen in the stem of the rice plant. The electrode was inserted into the stem of a live rice plant as shown in Fig. 4.5 (e). The control rice variety Nipponbare was used to measure the level of the dissolved oxygen in the stem. The locations are fixed at 1, 5 and 10 cm in stem of the live rice plant. The type-II oxygen electrode was inserted in each location at different depths of the stem. Therefore, the collected bacteria were cultured in the bacterial medium and then observed how bacteria survive at different state of the oxygen level.

Depending on the survival capability at the medium, then it will be released to the experimental pot of the rice plant. Then the growth rate of the rice will be observed at different days interval. For this purpose, the bacteria were cultured in the control and 21% oxygen containing media to observe the survival capability of the bacteria at different level of the oxygen. *Burkholderia vietnamiensis* is a nitrogen-fixing bacterium. It can secret EPS (external polymeric substances) in high-concentration of oxygen in the medium. EPS will not be secreted by the bacteria at low oxygen level. We want to observe which level of the oxygen is perfect for secreting the EPS. EPS secretion will be confirmed the activity of the bacteria in the media. All measurements were carried out at room temperature.

4.3 Results and discussion

4.3.1 Characterization of the needle types oxygen electrodes

Firstly, the electrochemical behavior of oxygen reduction in the miniature Clark-type oxygen electrode was investigated. Cyclic voltammograms of the bare platinum electrode was taken in electrolyte solution (0.1 M KCl solution) is shown in Fig. 4.6 (a) shows a typical cyclic voltammogram of oxygen reduction occurring in a miniature Clark-type oxygen electrode. The limiting current for oxygen reduction is observed to indicate that the reduction current measured in the region can be used to estimate the oxygen concentration.

The stability of the both types of the oxygen electrodes was also checked in an air saturated buffer solution at 25ºC for 2 h. The current was gradually drifted in negative direction to ensure the longer life time of the electrodes. The result of checking the stability is shown in Fig. 4.6 (b).

The response profile of the oxygen electrodes was obtained by changing the oxygen concentration between the air saturated state to the Na_2SO_3 saturated state. First, the electrode was immersed in distilled water to measure the stable current. Next, Na_2SO_3 was added, and the current was measured. The results of the reduction currents of the type-I and type-II oxygen-electrode has observed when the electrodes were applied at −0.8 V vs. cathode by the amperometry method. Fig. 4.7 (a-b) shows the typical response curves of the type-I and type-II oxygen electrodes, respectively. though the fabricated oxygen electrode is much smaller than the commercialized conventional oxygen electrodes, it showed clear, stable, reproducible responses. The 90% response time was less than 10 s for increasing changes and 50 s for decreasing changes. While conducting the experiments, however, an unnegligible residual current was detected.

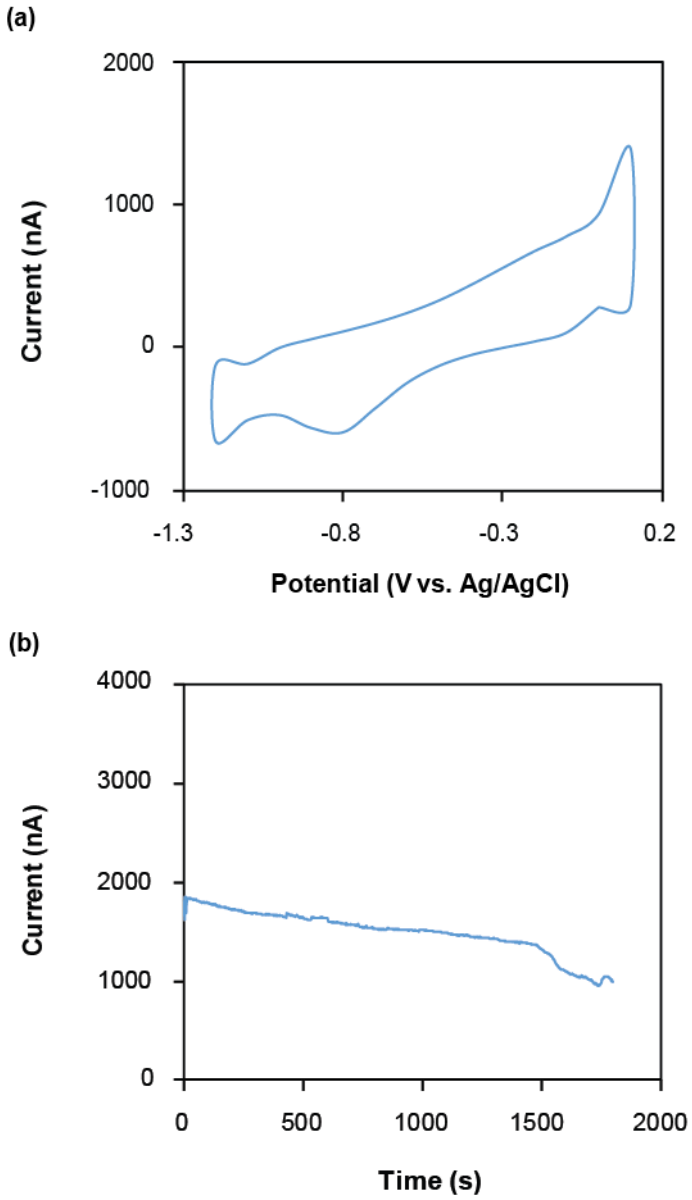

Fig. 4.6 The cyclic voltammogram and the stability of the type-I oxygen-electrode. (a) The cyclic voltammogram result of the bare platinum electrode. The scan rate was 100 mVs^{-1}. The total number cycle is 15. (b) The stability of the type-I oxygen electrode was checked in the in the 0.05 M buffer solution.

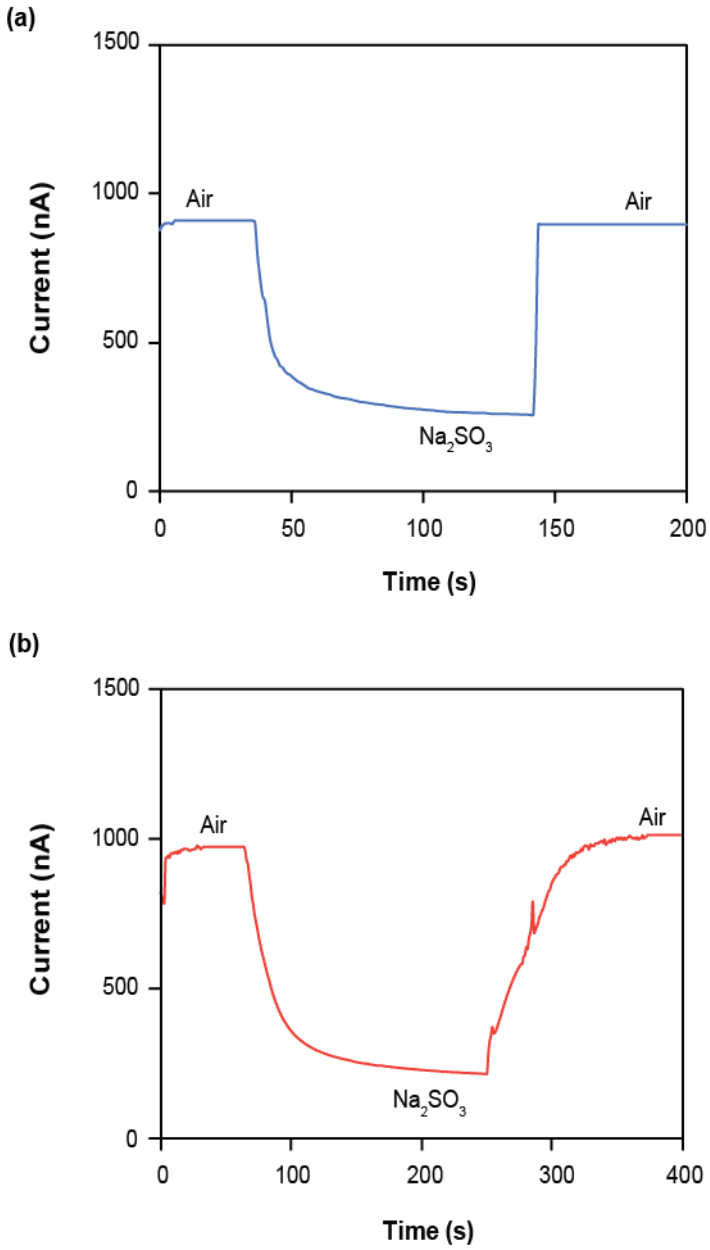

Fig. 4.7 Characterizations of the needle-type oxygen electrodes. (a) Response profile of the type-I oxygen electrode. (b) Response profile of the type-II oxygen electrode.

4.3.2 Measurement of the oxygen level in the bacterial medium

Some nitrogen-fixing bacteria has secreted the EPS in response to high O_2 concentration. We have checked the oxygen concentration in the liquid medium (0% O_2) (Fig. 4.8 (a)) and liquid medium (21% O_2) using the type-I oxygen electrode (Fig. 4.8 (b)). The approximately 15-hour bacterial culture medium was used for this experiment. The *Burkholderia vietnamiensis* bacteria was the culture in the medium. However, the electrode was inserted into the bacterial medium to record the current change at various depths of the medium. A 0 mm (surface), 1 mm, 2 mm, 3 mm and 4 mm depth of both medium has used for measuring the dissolved oxygen level.

The largest current was recorded at the 0 mm (surface) and the lowest current was recorded at 4 mm. The current was decreased with increases the distance from the surface to the depth of the sample. Also, the measured current in the liquid medium was found comparatively lower than the 21% oxygen medium. Because in the solid medium, the oxygen scavenging bacteria has used the oxygen for his survivability.

4.3.3 Measurement of oxygen concentration in the soil of rice root

The measurement of oxygen concentration in the rice plant root is important to know the better environment for the growth of nitrogen-fixing bacteria. Most of the nitrogen-fixing bacteria survive in the presence of oxygen. The type-I oxygen electrode was inserted into the soil of the around rice root system**.** The measured current was observed at the 0 mm (surface), 3, 7 and 10 mm depth of the soil. The highest current was observed at the surface and the lowest one was observed at the 10-mm depth of the soil (Fig. 4.9 (a)). The increasing and decreasing the current indicated the level of the oxygen.

4.3.4 Measurement of the oxygen level in the stem of the live rice plant

On the other hand, the type-II oxygen electrode was used to measure the dissolved oxygen level in live rice plants. A 1, 5 and 10 cm location of the stem have used for the measurement of the dissolved oxygen level. The locations were settled from the stem base. The current was measured in each location at the different depths of the stem i.e., 0 (surface), 1 and 2 mm. The 1 cm location has shown the highest current level rather than the others. In case of the depth measurement, the

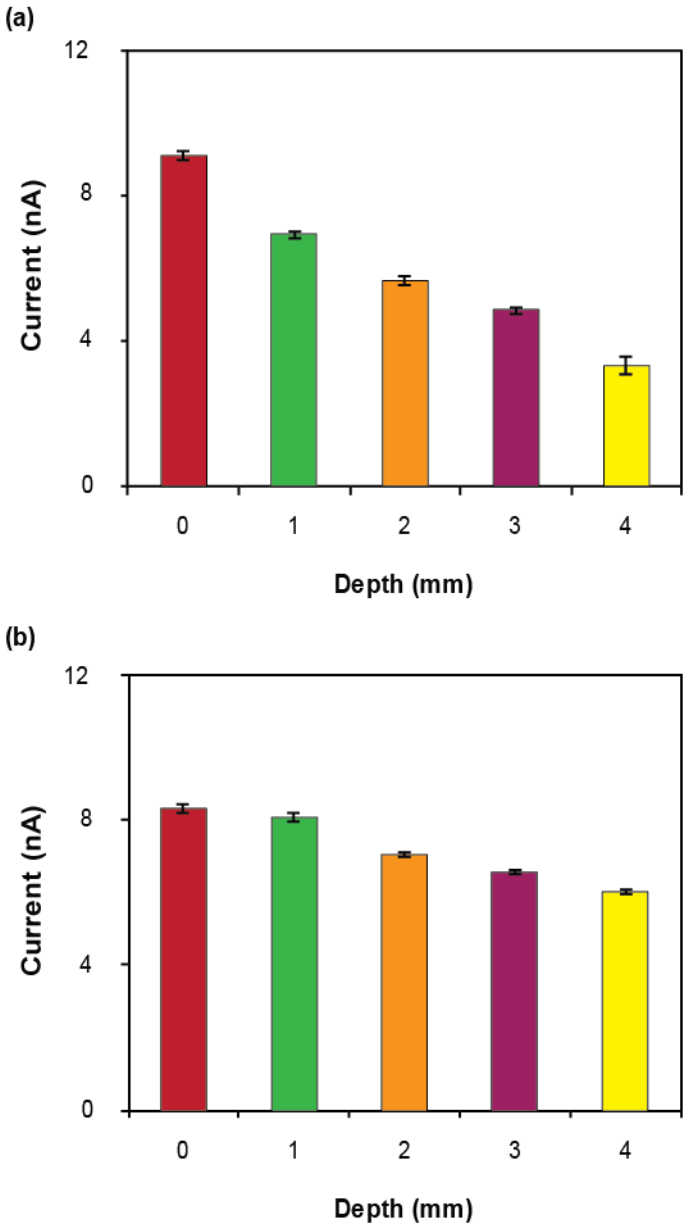

Fig. 4.8 The measurement of the oxygen in the medium. (a) The liquid medium contains 0% O_2. (b) The measurement of the dissolved oxygen level in the solid medium having 21% O_2 medium.

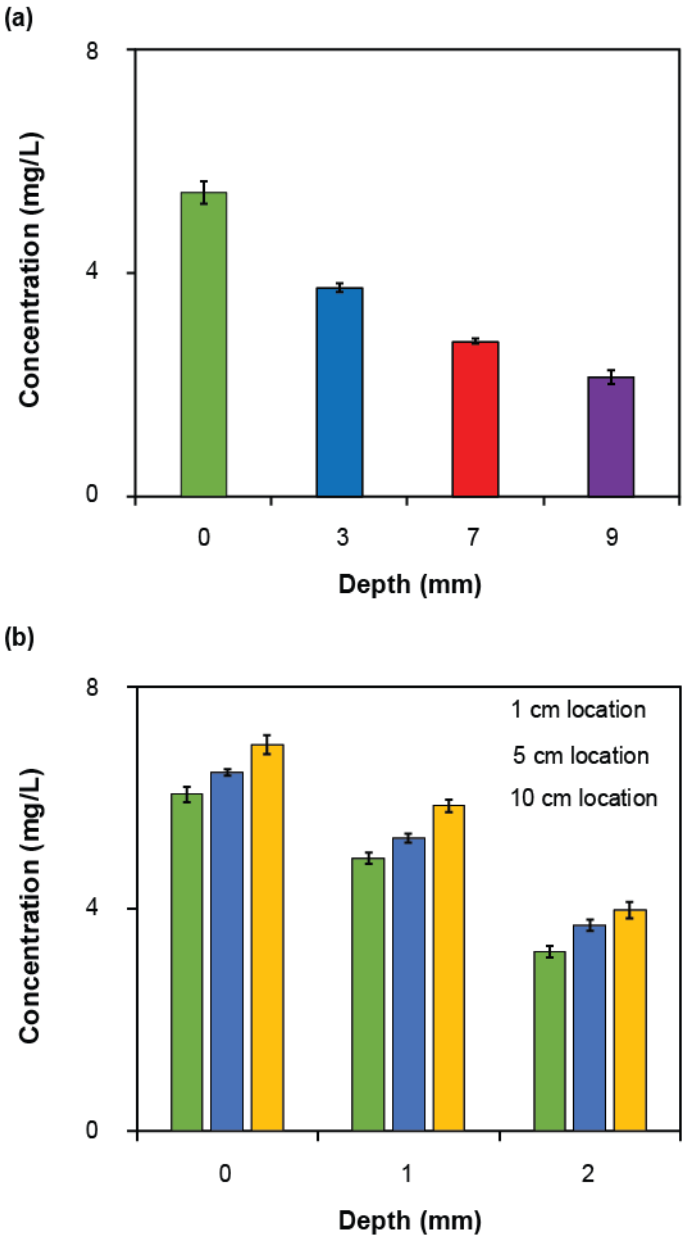

Fig. 4.9 Measurement of the dissolved oxygen level in the rice plant using the type-I oxygen electrodes. (a) The current changes were observed at the various depth of the soil of the rice plant. (b) The type-II oxygen electrode was used to measure the current changes in the various locations of the stem of the live rice plant.

surface has shown highest level of the oxygen rather than the 2-mm depth of the stem (Fig. 4.9 (b). The similar tendencies were observed in all location of the stem of the live rice plant.

4.4 Conclusion

Microfabricated Clark-type oxygen electrodes were demonstrated to measure the dissolved oxygen level in the salt stress plant. The type-I and type-II oxygen-electrodes were easily fabricated using sputtering and dicing process. Multiple numbers of oxygen electrode can produce through two batches of sputtering. Therefore, we can easily minimize the cost of fabrication rather than the previously reported fabrication of oxygen electrodes. The fabricated both type electrodes showed a sensitivity in the 1 mm length of the sensitive area. Depending on the research interest, the type-II oxygen electrode was also demonstrated due to its sharp end that could be beneficial to insert into the live plant. The fastest response time has been achieved for both electrodes compared with the previously reported electrodes.

References

1. G.S. Wilson: Bioelectrochemistry (Wiley, New York, 2002) pp. 40–46.
2. M. Koudelka: Sens. Actuators **9** (1986) 259.
3. H. Suzuki, E. Tamiya, and I. Karube: Anal. Chem. **60** (1988) 1080.
4. H. Suzuki, A. Sugama, and N. Kojima: Actuators B **2** (1990) 303.
5. H. Suzuki, N. Kojima, A. sugama, F. Takei, and K. Ikegami: Actuators B **1** (1990) 532.
6. H. Suzuki, N. Kojima, A. Sugama, and F. Takei: Actuators B **2** (1990) 191.
7. H. Suzuki, A. Sugama, and N. Kojima: Actuators B **10** (1993) 98.
8. Z. Yang, S. Sasaki, I. Karube, and H. Suzuki: Anal. Chim. Acta. **357** (1997) 49.
9. H. Suzuki, H. Ozawa, S. Sasaki, and I. Karube: Actuators B **54** (1998)146.
10. H. Suzuki, T. Hirakawa, S. Sasaki, and I. Karube: Chim. Acta **405** (2000) 65.

11. H. Suzuki, H. Arakawa, and I. Karube: Bioelectron. **16** (2001) 733.

12. H. Suzuki, T. Hirakawa, I. Watanabe, and Y. Kikuchi:Anal. Chim. Acta **431** (2001)259.

Chapter 5: Summary

In the objective of this study was to develop novel technique that may change the methodology of plant research.

In Chapter 1, the background of the study was introduced, and the objective of this study was mentioned.

In Chapter 2, a microdevice for the measurement of Na^+ ion concentration was described. The device was fabricated using a flexible polyimide film. Thin-film Ag/AgCl electrodes with a pinhole structure were used to improve stability. The pinhole structure was used to improve the stability of the Ag/AgCl electrode. A concentric platinum electrode was used for *in situ* growth of AgCl even after completing the device. The slope of the calibration plot was closed to that anticipated from the Nernst equation**.** Welsh onion was used to check the applicability of this device**.** It was found that the concentration was highest near to bulb area. Also, the salt concentration was found higher in all locations of salt exposed plant than control plant. For comparison, we also used a glass capillary ISE the similar tendency was observed as like as the microfabricated ISE.

In Chapter 3, needle-type ISEs for the measurement of the concentration of Na^+ and K^+ ions were introduced. The needle-type (type-I) and syringe needle type (type-II) was fabricated. The type-I ISE device was constructed with a polyimide film, silver, a PVP layer (act as an electrolyte layer) and a PVC layers as a reservoir for the ISEs. The polyimide film was used as a substrate considering the fabrication cost. The Ag/AgCl electrode was formed at one end of the silver layer (0.8 cm long) by depositing AgCl. To prepare the electrolyte solution, electrode was first coated with a PVP layer containing NaCl or KCl. The electrolyte layer was coated with a PVC layer**.** Finally, the ion-selective membrane was formed at the end of the needle end. The needle-type (type-I) polyHEMA junction RE was fabricated. The main difference in the electrolyte PVP layer. A 3 M KCl solution was used for making the electrolyte solution.

Depending on the experiment, the type-II ISEs and RE were fabricated. Components were incorporated in syringe needle (inner diameter: 0.9 mm). The ion-selective membrane and the liquid junction (poly(HEMA)) were formed at the sharp end of the syringe needle for the ISE and RE. The polyimide substrate with the Ag/AgCl electrode was inserted into the syringe needle. The electrolyte solution was introduced within the chamber**.** The fabricated ISEs were characterized using a

poly(HEMA) liquid junction RE and a commercial RE. In both case of ISEs, the slopes of the calibration plot were found close to the Nernst slope.

Next, the type-I ISE was used to measure the concentration of ions in a liquid sample, and the type-II ISE was used for direct measurement of concentration of ions in the stem of a live rice plant. It was found that Na^+ ion concentration was higher in the lower part of the stem than the upper part. On the other hand, K^+ ion concentration was higher in the upper part rather than the lower part. Also, the ion concentration was observed higher in the salt exposed rice plant than the control rice plant.

Chapter 4 describes the needle type (type-I) and syringe needle (type-II) oxygen electrodes were fabricated**.** Platinum and silver electrodes were formed on both sides of a polyimide substrate. The electrolyte layer was formed with the PVP solution. The chamber for the electrolyte layer was formed by coating the PVC layer. A 1 mm length of the sensitive area was formed at one end of the cathode and other parts was delineated with the polyimide layer. The end of the electrode was cut to form the oxygen-permeable membrane there.

Depending on the experiment, the oxygen electrode needs to be directly inserted into a plant. For this purpose, another type of oxygen electrode that employs a syringe needle (type-II) was fabricated. The type-II oxygen electrode is constructed with a syringe needle (inner diameter: 1.2 mm), electrolyte solution, anode, cathode and oxygen-permeable membrane. The polyimide string with the cathode and anode was also used to fabricate the type-II oxygen electrode. An oxygen-permeable membrane was formed at the sharp end of the syringe needle. To complete the oxygen electrode, a 0.1 M KCl solution was introduced into the syringe needle in a vacuum. The vacuum process was also effective to remove bubbles trapped in the sensing region.

The needle-type (type-I) oxygen electrode was inserted in the solution and gel sample. The current was observed higher in the liquid medium than the solid medium. Next, the type-I electrode was inserted in the different depth of the soil of the rice root system. Then, the current changes were observed at different depths of the soil. The current was observed higher at the surface of the soil than the longer depth. On the other hand, the type-II oxygen electrode was inserted in the different locations of the stem of the live rice plant. The current at 1 cm was higher than that of 5 cm and 10 cm. The type-II oxygen electrode was inserted at the 0 (surface), 1 and 2 mm depth of each location of the stem. We observed that the current became larger when the sensor inserted longer depth of the stem of the rice stem.

In this dissertation, some electrochemical sensors for the plant research were presented. These

sensors could be a milestone in agriculture to identify the salt tolerant and oxygen deficiency plant. Because the developed sensor is inexpensive, it can replace with the traditional large experimental setups. Needless to say, these sensors are applicable to other plants. We believe that the sensors will contribute to the basic researches of agriculture in the near future.

Appendix

Information of reagents, materials, equipment used for the fabrication, trial and evaluation of devices as well as experiments mentioned in chapter 2 to chapter 4 are summarized below.

Reagents and materials

- Polyimide sheet (130 μm thick) from JMT Corporation.
- Polyvinylchloride (PVC) sheet (120 μm thick) from As One Corporation.
- Soda lime glass capillaries (external diameter: ~1.8 mm, internal diameter: ~1.5 mm) from Asahi Glass.
- Positive photoresist (S-1818G) from Dow Chemical.
- Bis(12-crown-4) from Dojindo (Kumamoto, Japan).
- 2-nitrophenyloctyl ether (NPOE) from Dojindo (Kumamoto, Japan).
- Sodium tetraphenylborate from Sigma Aldrich (Buchs, Switzerland).
- Agarose S from Nippon Gene.
- Silver wire (diameter: 1 mm) from The Nilaco Corporation.
- Adhesive, Aron Alpha®, from Toagosei.
- PVC powder from Wako Pure Chemical Industries.
- Tetrahydrofuran (THF) from Wako Pure Chemical Industries.
- KCl from from Wako Pure Chemical Industries.
- NaCl from Wako Pure Chemical Industries.
- Milli-Q water from Millipore.
- Microposit developer (MF319) from Shipley.
- Acetone from Wako Pure Chemical Industries.
- Ethanol from Wako pure chemical industries.
- Toluene from Wako Pure Chemical Industries.
- 2-propanol from Wako Pure Chemical Industries.
- Silver nitrate from Wako Pure Chemical Industries.
- Low temperature agarose powder: Agarose-S from Wako Pure Chemical Industries.
- Polyvinylpyrrolidone (PVP) from from Wako Pure Chemical Industries.
- Poly(2-hydroxyethyl methacrylate) poly(HEMA) from Sigma Aldrich.
- Potassium tetrakis (4-chlorophenyl) borate from Sigma Aldrich.

- Dibutyl sebacate from Wako Pure Chemical Industries.
- A syringe needle (0.9 mm in inner diameter) from the Terumo.
- A syringe needle (1.2 mm in inner diameter) from the Terumo.
- Silicone adhesive (KE42) from Shin-Etsu Chemical.
- Welsh onion from local supermarket, Tsukuba, Japan.
- A Nipponbare rice variety from Japan.
- Bacteria (*Burkholderia vietnamiensis)* isolated from sweet potato.

Equipment's

- Sputter deposition equipment: CFS-4ES-231, Shibaura Eletec.
- Spin coater: 1H-D7, Mikasa.
- Mask aligner: MA-10, Mikasa.
- Dicing equipment: A-WD-10A, Tokyo seimitsu.
- Dry oven: OF-450, AS ONE.
- Hot plate: ND-1, AsOne.
- Pure water manufacturing equipment: Direct Q 3 UV with pump, Millipore.
- Potentiostat/galvanostat: HA-151, Hokuto denko.
- Potentiostat/galvanostat: PGSTAT12, Autolab, Eco Chemie.
- Thermostatic bath: WBS-80A, As one.
- Microscope: SMZ1500, Nikon.
- Digital cameras: NEX-5N, Sony.
- Laser microscope: VK-8510, Keyence,
- Entity fluorescence microscope system: VB-G25, Keyence.
- Fluorescence microscope: IX-73, Olympus, Japan
- Silver / silver chloride reference electrode: # 2080A-06T, Horiba.
- Ag/AgCl reference electrode # 2060A, Horiba.
- Mask drawing software: Adobe illustrator CS6, 2015.
- Sandblaster: SG 106, Hozan Tool Industries Company Limited.

Fabrication of the electrochemical sensors

1. Sand blasting of the polyimide substrate

A polyimide sheet was used for sand blasting. The surface of the sheet was made rough using the sand blaster. The rough surface increases the adhesion of the metal with the base polyimide layer.

2. Cleaning of the substrate

The substrate was cleaned with distilled water and acetone using a magnetic stirrer. The substrate was further cleaned three times in acetone using a sonicator for 15 min in total (5 min × 5 min × 5 min). Fresh acetone was used each time.

3. Lift-off process

The electrodes were formed by a thin-film process. A 30-nm-thick chromium layer and a 300-nm-thick platinum layer were sputter-deposited in this order on the polyimide base layer after the formation of positive photoresist patterns, and the electrode patterns were formed by lift-off. The chromium layer was used to promote the adhesion of the platinum layer to the base layer. Then, 600-nm-thick silver patterns were formed only on the two circular platinum areas by lift-off in the same manner.

4. Formation of the pinhole structure and insulating layer for the microfabricated Na^+ ion-sensing device

The positive photoresist was used for insulation and three pinholes of 40 μm diameter were formed on each circular silver electrode**.** The thickness of the insulating layer was 2.7 μm.

5. Forming the Ag/AgCl electrode for the microfabricated Na^+ ion-sensing device

A 100 mM KCl solution was placed on the silver pattern and the concentric platinum pattern, and AgCl was grown from the pinholes into the silver layer by applying a constant current (50 nA) for 10 min using a galvanostat (HA-151, Hokuto Denko, Japan). After the device was completed and used for experiments, AgCl was additionally grown using the internal electrolyte solution (1.0 M KCl) by applying 50 nA for 5 min in the same manner to guarantee the stable potential of the Ag/AgCl electrode.

6. Forming the liquid junction for the microfabricated Na^+ ion-sensing device

To make the liquid junction for the RE, a 2% agarose gel solution was prepared with a 1.0 M KCl solution. The solution was heated on a hot plate for 30 min at 90 °C and was injected into the other through-hole of the PVC layer without the ion-selective membrane after bonding the PVC layer to the second polyimide layer.

7. Preparation of the sodium ion selective membrane solution

For the Na^+ ion-selective membrane, crown ether is a representative ionophore. To form the membrane, 101 mg of PVC powder was dissolved in 3 mL of THF. Then, 200 µL of NPOE, 10 mg of bis(12-crown-4), and 6 mg of sodium tetraphenylborate were added.

8. Formation of the dry electrolyte layer and ion-selective membrane for type–I ISE

To prepare the electrolyte solution for the sodium ion-selective electrode, a 75 % PVP solution was prepared by dissolving the PVP powder in a 0.1 M NaCl solution. The Ag/AgCl part of the electrode was immersed in the 75% PVP solution and was removed from the solution immediately. The dry PVP layer was obtained after drying for 30 min. The dry PVP layer was obtained after drying for 30 min. THF was used as a solvent for making a 66% PVC solution. The electrode with the PVP layer was immersed in the PVC solution to make the reservoir of the electrolyte layer. The PVC-coated electrodes were dried for 10 min. After forming the electrolyte chamber, the end of the Ag/AgCl electrode was cut using a scissor. The sodium ion-selective membrane was formed at the end by immersing the part in the sodium ion-specific ionophore solution. The membrane was formed after drying for 24 h.

9. Preparation poly(HEMA) solution for the needle-type reference electrode (RE)

To prepare the liquid junction for the type-I and type-II RE, a 0.05M poly(HEMA) powder was dissolved in the ethanol as solvent. The solution was thoroughly stirred to mix properly. The type-I RE electrode end and the sharp end of the syringe needle were dipped in the poly (HEMA) solution to form the liquid junction. The liquid junction was inserted five times in poly(HEMA) solution and was removed immediately. Finally, the liquid junction was formed after drying for 24 h. To complete ISEs and RE devices, a 0.1 M NaCl for the sodium ion-selective electrode (type-I and type-II), 0.1 M KCl solution for the potassium ion-selective electrode (type-I and type-II), and 3 M KCl solution for the type-I and type-II RE were used as electrolyte solution.

10. Patterning of the protective layer for the oxygen electrode

To form the protective layer, the polyimide prepolymer solution was spin-coated and was baked for 30 min at 80 °C. Next, a positive photoresist was spin-coated and was baked for 30 min at 80°C. The polyimide substrate by placing the printed designed mask and exposing it to ultra violet light emitted from the mask aligner for 40 s. The photoresist was developed in a developer solution for 1 min. After that, the substrate was rinsed with distilled water for 1 min and in ethanol for 2 min. Finally, the substrate was cured at 150 ^{o}C for15 min, at 200 ^{o}C for 15 min, and at 280 ^{o}C for 30 min.

11. Cleaning of the syringe needle

To form the oxygen-permeable membrane, the syringe needle was cleaned with 99.99% ethanol for 10 min using a sonicator. Next, the syringe needle was dried on a hotplate for 20 min at 120 ^{o}C. The sharp end of the syringe needle was inserted in a silicone adhesive to form the oxygen permeable membrane. The membrane was used for the experiment after drying it 24 hours.

12. Introduction of the electrolyte solution within chamber

The electrolyte solution has taken into the centrifuge tub. A Ag/AgCl electrode was incorporated in the syringe needle. Then, the syringe needle was vertically inserted in the centrifuge tube. Next, the tube with electrode was placed into the vacuum chamber and was removed the bubble. Therefore,

the electrolyte solution was introduced within the needle chamber. Sometimes, these steps were followed two or three times depending on the requirements, but maximum cases one time was followed.

13. Formation of oxygen-permeable membrane

The end of the syringe needle and needle-type oxygen electrode was inserted in the silicone adhesive, to form the oxygen-permeable membrane. The oxygen-permeable membrane was formed after drying for 24 h.

14. Making the electrical connection for the electrodes

To make the electrical connection to the electrodes, the aluminum foil insulated side of the alligator clip was connected to the either anode or cathode. While the aluminum foil side of an alligator clip was connected to the cathode and polyimide tape wrapped side connected to the anode, then it was act as a connector for the cathode. Similarly, while the aluminum foil insulated side of an alligator clip connected to the anode and polyimide tape wrapped side connected to the cathode, then it was act as connector for the anode. Finally, the other end of an alligator clip was connected to the potentiostat.

15. Dicing and sputtering

The electrode was prepared by sputtering and then dice. After dicing the multiple number of polyimide string obtained.

List of publication

Md. Abunasar Miah and Hiroaki Suzuki. Disposable Na^+ Ion-Sensing Device for Research on Salt-Tolerant Plants. Sensors and Materials. **30 (1)** (2018) 119-127.

List of conference

Md. Abunasar Miah, Masatoshi Yokokawa, Edwin T. Carlen, and Hiroaki Suzuki, "Direct Measurement of Na^+ Ion Concentration in Live Plants Using Miniaturized Ion-Selective Electrode (ISE)", *6th Anniversary, Interdisciplinary Workshop on Science and Patents (IWP), University of Tsukuba, Tsukuba, Ibaraki, Japan*, 2017.

Acknowledgements

I would like to express my sincere gratitude to my supervisor, Prof. Hiroaki Suzuki (Graduate school of pure and applied science, institute of Materials Science, University of Tsukuba, Japan) for his continuous support, patience, motivation, enthusiasm, and immense knowledge of my Ph.D. study and related research. Planning and conducting my experiment together with writing my doctoral thesis would not have been possible without his kind support. I have benefited immensely, both scientifically and personally, from my time under his mentorship.

I would like to convey my heartfelt thanks to the Japanese government (Ministry of Education, Culture, Sports, Science and Technology, Monbukagakusho) for financially supporting to my study.

My genuine thanks also go to Professor Edwin T. Carlen. He has constantly mentored to carry out the research. He is a beloved person myself who motivated me not only for research purpose but also made a sort of discussion when I felt stress. I wish a healthy life of Professor Edwin T. Carlen.

Besides my advisor, I would like to express the heartiest gratitude to Associate Professor, Masatoshi Yokokawa for his numerous supports and positive attitudes throughout my research. I would also like to thank Professor Motohiko Kondo of Nagoya University, Japan, for valuable information and advice on the studies related to the plants. I would also like to thank all lab members of the Professor Motohiko Kondo laboratory for their valuable discussion related with the experiment in rice plants.

Special thanks go to all my ‘Suzuki-Yokokawa’ laboratory members for their valuable support regarding the research and life style in Japan. Especially, I would like to thank Mr. Isa Anshori for his kind support and sleepless working nights passed together before deadlines of the Ph.D. dissertation.

I would also like to thank Mr. Tanabe who help me to learn basic experiments at the beginning of my study. Also, my tutor Mr. Suzuki who help me to know the Japanese culture, education and some places of the Tsukuba that made my life easy during his tutorship.

Finally, the deepest and boundless gratefulness goes to my parents and two sisters. Without their kind support and motivation, higher study is impossible to get and finish until the intended destination. I would like to thank my relatives, well-wishers, friends, colleagues for their cooperation. I am heartedly grateful to my loveliest wife “Ummay Salma Khatun (Pushpo)” for her endless patience, mental support and inspiration during my study period. Without my family support, I never able to reach this dream successfully.